



Review

A review of spherical triboelectric nanogenerators for harvesting high-entropy ocean wave energy

Junjie Cui^{a,1}, Hao Li^{b,c,1}, Baodong Chen^{b,c,*}, Zhong Lin Wang^{b,c,d,*}

^a Inner Mongolia Key Laboratory of Advanced Ceramic Materials and Devices, Inner Mongolia University of Science and Technology, Baotou 014010, PR China

^b Beijing Institute of Nanoenergy and Nanosystems, Chinese Academy of Sciences, Beijing 101400, PR China

^c School of Nanoscience and Engineering, University of Chinese Academy of Sciences, Beijing 100049, PR China

^d Georgia Institute of Technology, Atlanta, GA 30332-0245, USA

ARTICLE INFO

Keywords:

Spherical triboelectric nanogenerator

High-entropy

Ocean wave energy

Self-powered system

ABSTRACT

Triboelectric nanogenerators (TENGs) with the merits of low-cost, environmental friendliness is the most widely used and regarded as an innovated technology of harvesting high-entropy ocean wave energy (HE-OWE), considering as one of the promising sustainable and cleanable energy sources, which TENG with spherical structure is more favorable. This review mainly focuses on the recent advances of spherical (S)-TENGs for harvesting HE-OWE and self-powered system due to the absolute advantages of simple structure and fabrication more easily. From the perspective of working modes of S-TENGs in different ocean occasions, in-depth research on the relationship between triboelectric material properties, structural characteristics, and the electrical output performance of devices are compared for high efficiency development of HE-OWE. These S-TENGs shows the great potential for driving marine electronic devices and boosting the rapid development of marine economy inevitably. Furthermore, the potential values are explored and tough challenges that can impede their large-scale commercial applications are discussed.

1. Introduction

With the invention of steam engine for the first industrial revolution, the energy demands of traditional non-renewable fossil fuels are growing continuously and further the energy are exhausted [1]. And quick development of traditional industry has prompted human beings to explore new energy sources to meet the growing energy demand [2]. In the recent decades, the researchers witnessed the renewable energy sources such as solar energy [3], wind energy [4], and tidal energy [5], and they have been extensively applied in our life. Unfortunately, these kinds of sustainable and clean energy depended too much on external factors such as rigid texture, sunlight, temperature, etc., making them difficult to be effectively utilized on a large scale. Moreover, many inherent shortcomings, such as limited storage capacity, frequent charging, limited services life, serious environmental hazards, etc. restrict the real application of conventional devices rigid battery [6], rechargeable battery [7], electrochemical capacitor [8], and so on. Thus, development of sustainable, renewable and clean energy is an inevitable trend that all of the world has to be met. From the perspective of the

long-term, cost-effective, environmental friendliness of power source, power acquisition directly from the surrounding environments is the ideal choice for distributed power supply and self-powered sensing system.

Entropy is a measure of the degree of system disorder, defining as the one of the parameters representing the state of matter in thermodynamics. It is divided into high entropy energy and low entropy energy with this concept applied in the field of energy. Compared to the low entropy energy source with high frequency and highly order, high entropy energy exhibits the characteristics of low frequency and highly disorder. Except for the former, HE-OWE possesses the merits of huge amounts, environmental friendliness, predictability and consistency as well as high energy density [9–11], as illustrated in Fig. 1. Furthermore, characteristic wave of ocean contains capillary wave, break wave, gravity wave, interfacial wave, internal wave, shallow water wave, deep water wave. It is estimated that covering area of ocean on earth surface is more than 70.8 %, predicting that high-entropy ocean wave energy (HE-OWE) is the total reserves of wave energy around coastlines exceeding 2 TW (1 TW = 10^{12} W) [12,13]. The successful

* Corresponding authors at: Beijing Institute of Nanoenergy and Nanosystems, Chinese Academy of Sciences, Beijing 101400, PR China.

E-mail addresses: chenbaodong@binn.cas.cn (B. Chen), zlwang@gatech.edu (Z.L. Wang).

¹ these authors contributed equally to this work.

implementation achieving the conversion from HE-OWE into electricity has received considerable research interests of many of researchers in the world [14–16]. Nevertheless, there still exists the apparent demerits in Fig. 1, such as random-uncertainty, low-frequency and low-amplitude, in which these demerits will bring about many difficulties in harvesting HE-OWE [17–21], especially the issue of low capture efficiency. Thereby, improving the capture efficiency is a primary work for impelling development of HE-OWE. It is an effective way of settling the issue concerning global climate warming.

In the past decades, electromagnetic generators (EMG) have been used to harvest low-frequency HE-OWE [22–27]. Unfortunately, inefficient performance for EMG is noticed owing to the application occasions of harvesting high-frequency mechanical energy and it has the inherent characteristics, i.e., heavy weight, bulk mass, high cost, harsh application environment [28,29]. piezoelectric nanogenerator (PENG) has ever been used to harvest low frequency mechanical energy. PENG employs the piezoelectric polarization charges and the generated electric field with the time varied to drive the electrons to flow through the external circuit. The produced voltage is equivalent to the values of pressure or tension imposed on the crystal. The polarization charge density is increased by enhancing the applied force and the electrostatic potential created by the polarization charges is balanced by the flow of electrons

through electrodes. The present limitation of piezoelectric harvesters is their high impedance which lessens the accessible current. Thus, it is urgent to explore a novel method to harvest HE-OWE effectively on a large-scale. With the advances of nanotechnology, a kind of mechanical energy harvester, namely triboelectric nanogenerator (TENG), was first proposed in 2012 by Wang based on the coupling of triboelectrification effect and electrostatic induction [30–32]. Output current of TENG results from displacement current of Maxwell equation [33–38]. Excitedly, the fundamental theoretical origin has been established [39,40], indicating that the TENG is not only a practical technology, but also a research discipline. Compared to the EMG, TENG possesses the advantages of light weight, low-cost, high-power density, simple structure, environmental friendliness and fabrication easily [30,41–43], which is regarded as a greatly desired as a key to harvest HE-OWE under arbitrary frequency at the random direction [44–47]. Besides, it can provide the self-powered power source for various marine environmental monitoring, weather forecasting, navigation, buoy floating on the ocean, artificial intelligence, wireless communicative devices and internet of things or the other electronic device that can boost the development of marine economy [31,48–57].

According to fundamental working modes, the multifarious kinds of TENGs for harvesting HE-OWE, as shown in Fig. 2. The F-T-L working

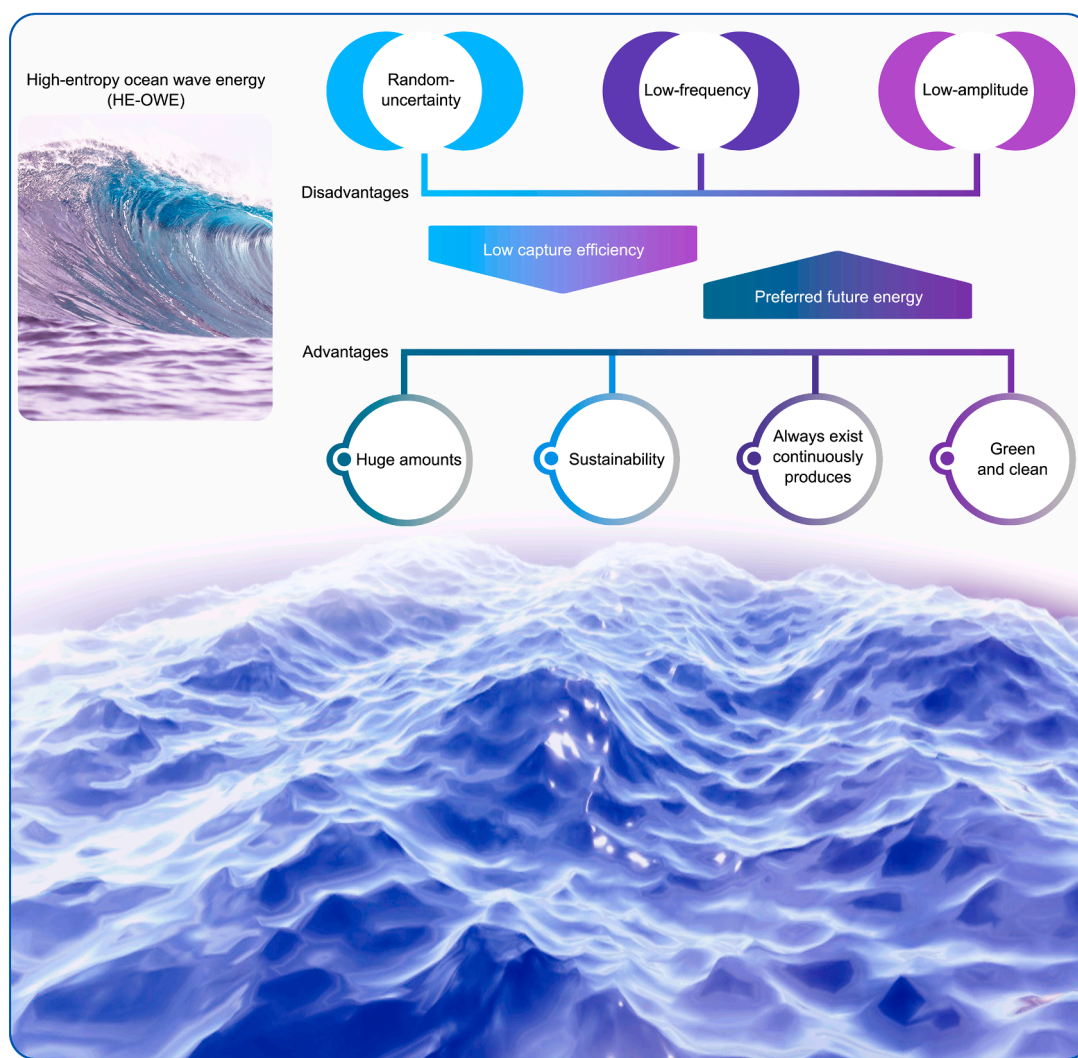


Fig. 1. Illustration of advantages and disadvantages for low-grade ocean wave energy as well as characteristic wave. The advantages contain huge amounts, sustainability, always exist and continuously produces along with green and clean. The disadvantages include the random-uncertainty, low-frequency and low-amplitude. Characteristic wave comprised the characteristics of capillary wave, break wave, gravity wave, interfacial wave, internal wave, shallow water wave and deep water wave.

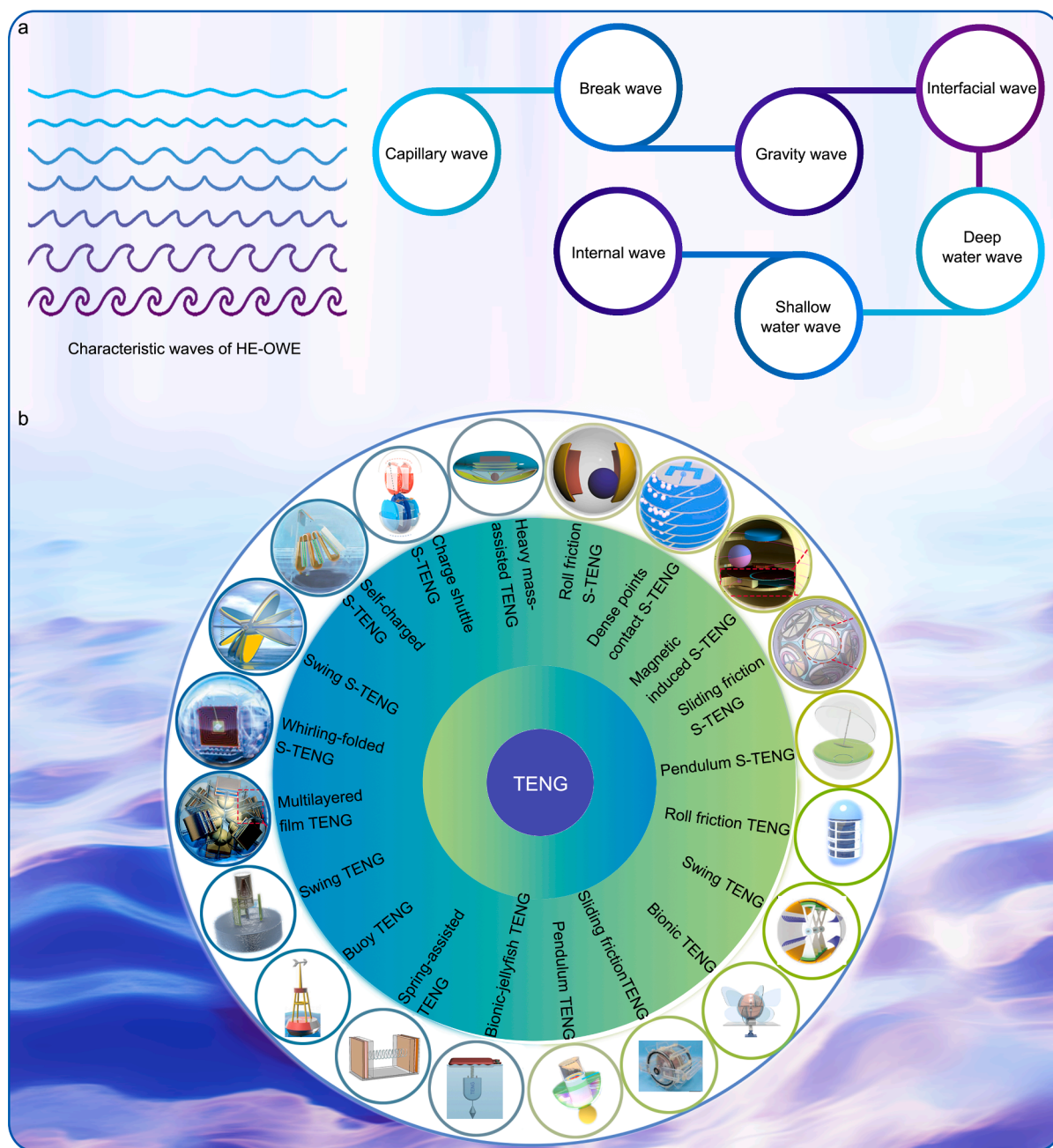


Fig. 2. Classification of multifarious kinds of TENGs according to fundamental working modes. All the Figures are reproduced with permission. [31,46,55,61,69,71,78,8,22,90,97,103,107,106,113,114,116,111,118] and [119] Copyright, 2017, 2018, 2019, 2020, 2021, 2022, 2023, American Chemical Society, Elsevier, Nature, Wiley-VCH, Royal Society of Chemistry.

mode include the types of pendulums [22], butterfly [58], swing [59–62], friction [63,64], dense point contact [13,65], etc. [66–68], whereas the C-S working mode contains bionic-jellyfish [69], spring-assisted [70,71], buoy [72], multilayered film [73], wavy-structured [74], and so on [75,76]. No matter what the inner structure is, it complies with the contact electrification and electrostatic induction, which the relative displacement that is perpendicular/parallel to electrode interface occurs between dielectric layer and metal electrode layer or between dielectric layer, leading to pump potential difference of electricity induced by the difference of electronegativity. For the latter, electrostatic induction are yielded as the dielectric layer covering on the metal electrode layer is charged with the process of contact electrification generating between dielectric layers. Thus, the flow of electrons is created in an alternative manner and obtained by the external loading

circuit. In addition to this, the exteriors of TENGs are in diversity of cylinder shape [77,78], polyhedral shape [79], gear wheel shape [80], duck shape [35], torus shape [72], arc shape [81], tetrahedral shape [82], disc-like shape [83], bionic-jellyfish shape [84–86] and spherical shape, etc. [87–89]. Particularly, the integration of advanced low-frequency mechanical energy harvesting technologies inside the hollow sphere contributes to the emergence of a new kind of TENGs, namely spherical (S)-TENGs [90,91]. With the help of S-TENGs, it can convert HE-OWE having the characteristics of low-frequency and low-amplitude into electrical output under arbitrary frequency from any direction and apply it in a self-powered system in the ocean. More importantly, S-TENGs have the irreplaceable unique merits of better applicability, broader application, integration easily, simple structure, infinite inner structure design, highly attractive technology compared to

the other kinds of TENGs with a non-spherical exterior. It is deeply believed that the deepen research of HE-OWE will be boosted by using S-TENGs and even more marine resource will be developed in future. Notwithstanding, several fundamental issues are still not comprehensively overviewed and have to be corrected together, which bound the commercialized development.

Several researches have been detailedly conducted on S-TENGs in harvesting HE-OWE in until up to now. However, the review concerning the development of S-TENGs for harvesting HE-OWE and self-powered sensing in the aspect of exploiting the marine resources is relatively limited, particularly the present and potential applicable scenarios of S-TENGs. S-TENGs possess the absolute advantages in low-cost, simple structure, fabrication more easily, environmental friendliness, and so on. However, S-TENGs are not being used more widely. Herein, we cover recent advances in S-TENG, including the common characteristics of existing inner structure, materials selection, output performance and applicable scenarios. Impacting factors for the output performance of S-TENG-based network are analyzed. The different applicable scenarios are overviewed according to the merits and demerits of S-TENGs in harvesting HE-OWE and self-powered sensing. It is recommended that charge injection by using pump-TENG in limited space of S-TENG can improve the output performance. It is anticipated that the related researchers and developers are greatly benefited from this paper and a specific direction of developing prospects in this field are provided.

2. Structure and working modes of TENGs

Fig. 3 shows four fundamental working modes of TENGs and the statistic results of various appearance structure in the field of harvesting HE-OWE. It is well-known that the TENGs are divided into four fundamental working modes based on electrode configurations and working

mechanism, including contact-separation (C-S) mode, lateral-sliding (L-S) mode, single-electrode (S-E) mode and freestanding triboelectric-layer (F-T-L) mode. As shown in Fig. 3a, C-S mode relies on the relative motion between triboelectric layers and metal electrode being perpendicular to the interface, having the structural characteristics of contact area and separated distance. There exhibits many structural characteristics for L-S mode that are simple structure, horizontal movement being parallel to interface, no air gap. For S-E mode, it shows the simplest structure, integration more easily and one electrode connected to ground. Comparably, there shows the relative movement of dielectric layers composed of polymer materials between two metal electrodes for F-T-L mode, regarding as the improved mode of S-E mode. It has in the virtue of high sensitivity, long service life and easy to fabricate.

It is noted that spherical TENG in Fig. 3b possess the highest percentage, 28.2%, indicating that the spherical TENGs have attracted the extensive attention due to the irreplaceable merits of wide applicability, broader application, integration easily, simple structure, infinite inner structure design, and highly attractive technology. We find in Fig. 3c that the percentages of the commonly used fundamental working modes of S-TENGs are 67.7% and 32.3% for F-T-L and C-S working modes, respectively, according to the results of Fig. 4 and Fig. 5, implying that these two working modes are suitable for the S-TENG. They possess the common advantage of easy to fabricate, high electric output, slight interfacial abrasion and no grounding electrode that is suitable for harvesting HE-OWE. These two working modes are affected by the contact interface, velocity and separation clearance. No matter which working mode, it complies with the basic principle of the charged contact of water and dielectric materials.

Resulting from the working mechanism of TENG, water itself is regarded as the triboelectric materials with the cooperation of

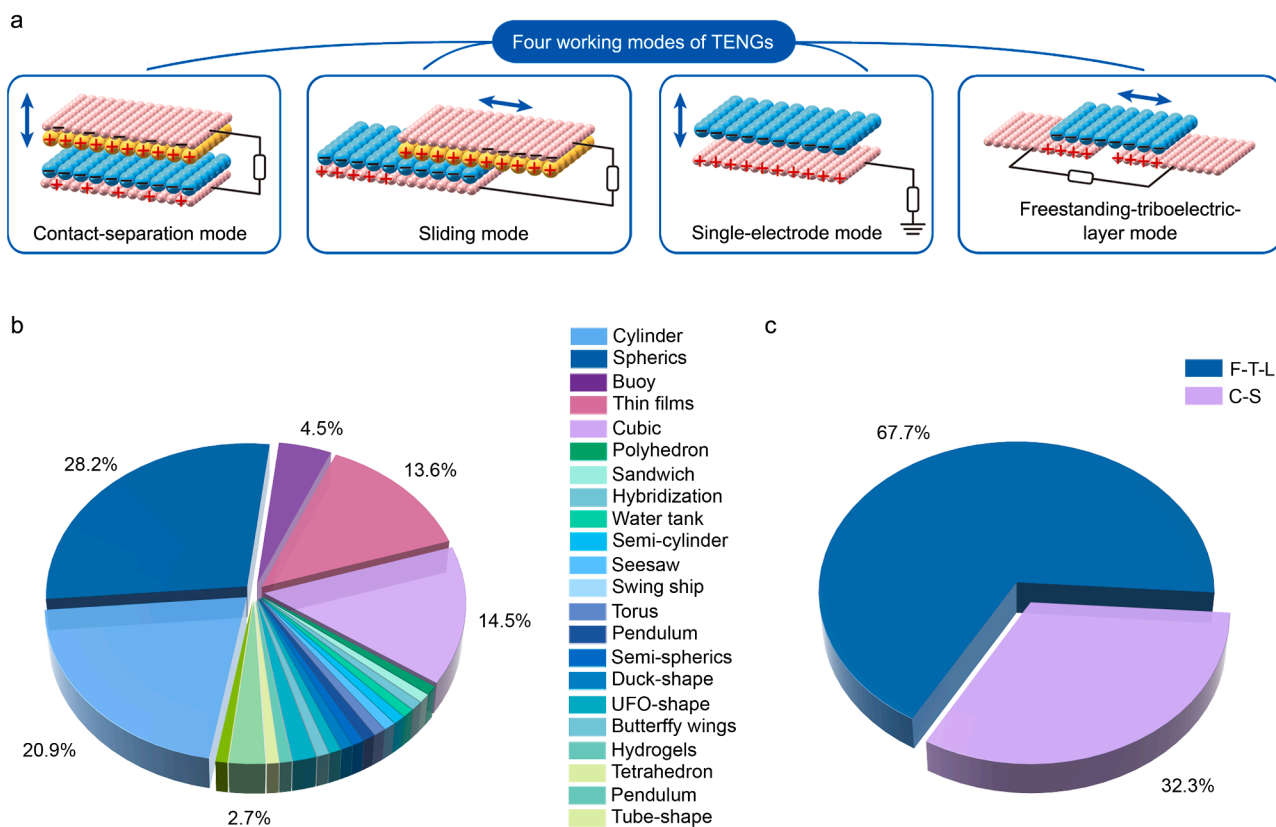


Fig. 3. Four fundamental working modes of TENG and percentage of S-TENG with various exterior and different fundamental working mode. (a) Four working modes of S-TENG, including contact-separation mode, lateral sliding mode, single electrode mode and freestanding triboelectric layer mode. (b) Percentage of several S-TENG with the various exterior applying HE-OWE. (c) Percentage of several S-TENG with the working modes applying HE-OWE.

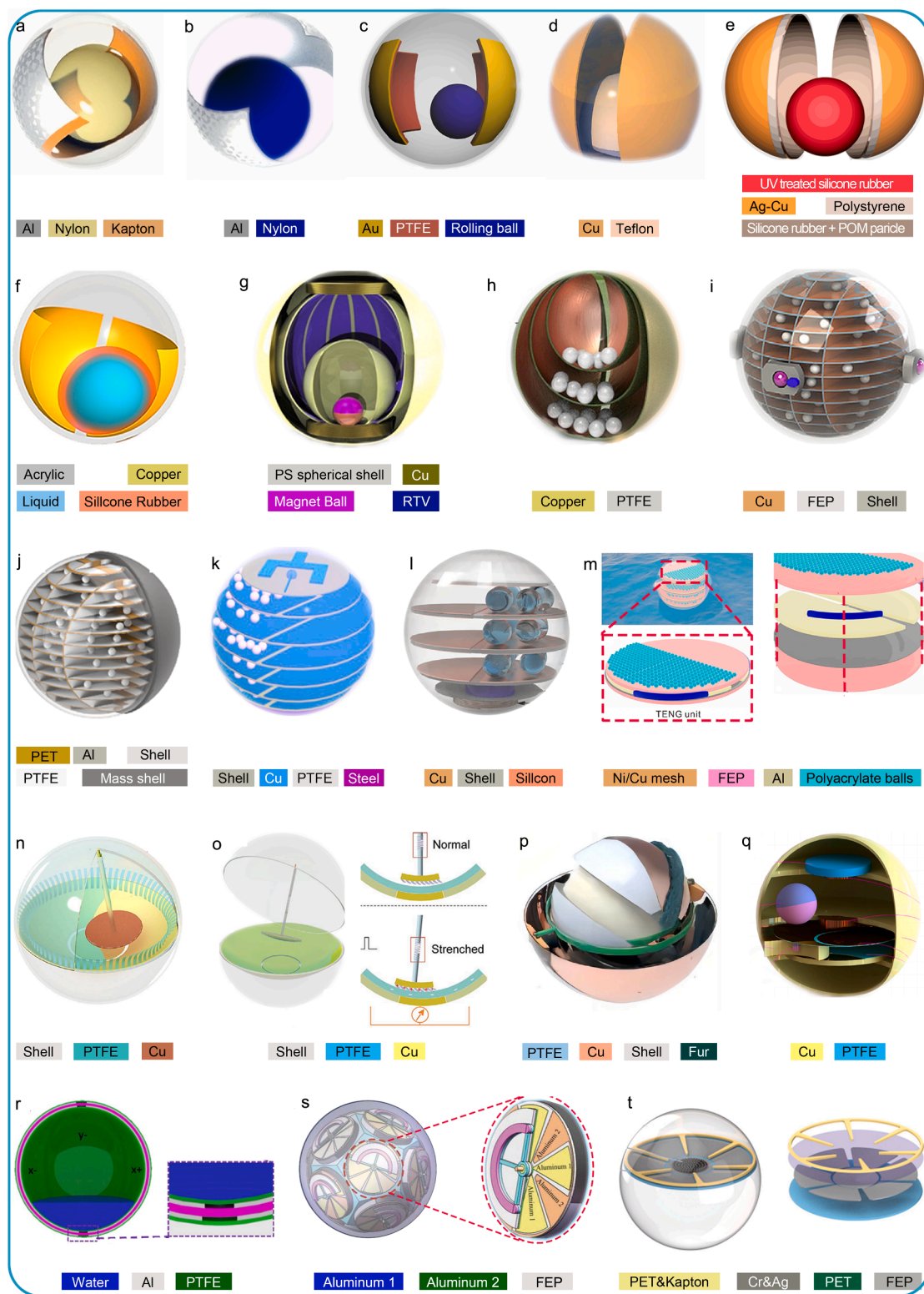


Fig. 4. Inner structure of all kinds of S-TENG with F-T-L working mode. (a), (b) Reproduced with permission. [91] Copyright 2015, Wiley-VCH. (c) Reproduced with permission. [90] Copyright 2021, American Chemical Society. (d) Reproduced with permission. [92] Copyright 2020, Cell. (e) Reproduced with permission. [94] Copyright 2018, American Chemical Society. (f) Reproduced with permission. [93] Copyright 2019, Elsevier. (g) Reproduced with permission. [99] Copyright 2020, Elsevier. (h) Reproduced with permission. [101] Copyright 2019, Elsevier. (i) Reproduced with permission. [100] Copyright 2019, Elsevier. (j) Reproduced with permission. [96] Copyright 2023, Royal Society of Chemistry. (k) Reproduced with permission. [97] Copyright 2023, Elsevier. (l) Reproduced with permission. [95] Copyright 2023, Wiley-VCH. (m) Reproduced with permission. [98] Copyright 2021, American Chemical Society. (n) Reproduced with permission. [102] Copyright 2019, Elsevier. (o) Reproduced with permission. [103] Copyright 2021, Wiley-VCH. (p) Reproduced with permission. [105] Copyright 2022, American Chemical Society. (q) Reproduced with permission. [107] Copyright 2019, American Chemical Society. (r) Reproduced with permission. [108] Copyright 2017, Elsevier. (s) Reproduced with permission. [106] Copyright 2022, Wiley-VCH. (t) Reproduced with permission. [104] Copyright 2023, Elsevier.

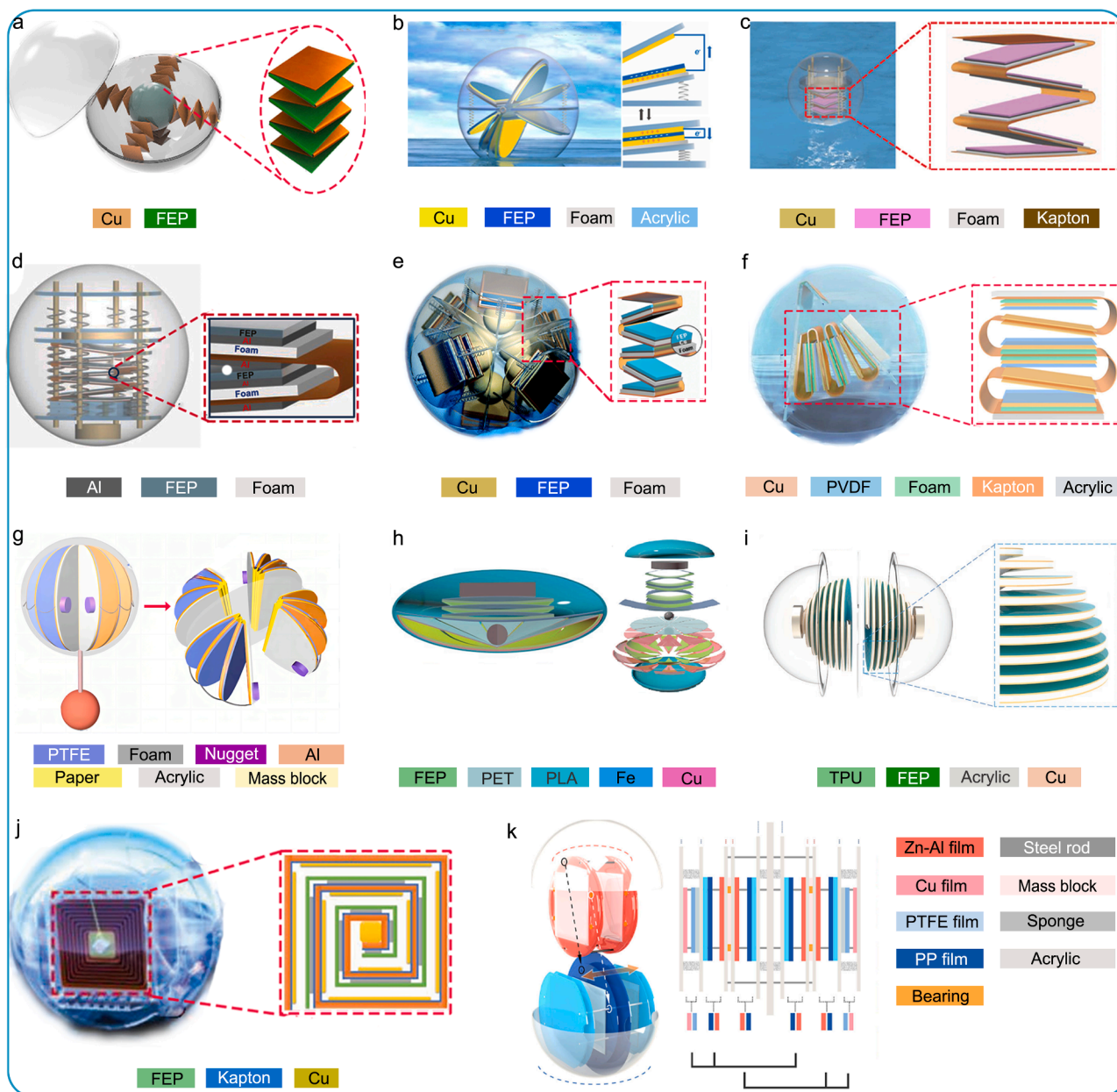


Fig. 5. Inner structure of all kinds of S-TENG with C-S working mode. (a) Reproduced with permission. [109] Copyright 2020, Elsevier. (b) Reproduced with permission. [113] Copyright 2021, Elsevier. (c) Reproduced with permission. [117] Copyright 2018, Wiley-VCH. (d) Reproduced with permission. [115] Copyright 2019, Wiley-VCH. (e) Reproduced with permission. [114] Copyright 2020, Royal Society of Chemistry. (f) Reproduced with permission. [116] Copyright 2019, Wiley-VCH. (g) Reproduced with permission. [112] Copyright 2022, Elsevier. (h) Reproduced with permission. [111] Copyright 2023, Elsevier. (i) Reproduced with permission. [110] Copyright 2023, Wiley-VCH. (j) Reproduced with permission. [118] Copyright 2019, Wiley-VCH. (k) Reproduced with permission. [119] Copyright 2020, Springer Nature.

hydrophobic and insulated polymer materials. As the repetitive emerging-submerging process with the interaction between traveling water waves and the TENG, charges are yielded resulting from the existence of contact electrification and electrostatic induction, that the water drops and dielectric materials have the same amount of charge and opposite charges on its surface because of the friction with dielectric materials. Meanwhile, tribo- and induced-charges are transferred due to a potential difference created between the Cu electrode and ground, driving the electron transfer from ground to the Cu electrode. Once the water drop moves off the dielectric surface, an opposite electric potential difference induces the electrons to flow back. This is the current generation process of typical interaction between water and hydrophobic and insulated polymer materials.

As shown the F-T-L working mode in Fig. 3a, it is composed of one triboelectric layer and two electrodes, that the horizontal movement of dielectric layer is along the two electrodes. Fig. 4 exhibits the specific examples of S-TENGs with the various inner structure of complying with the F-T-L working mode, in which the common characteristics are one triboelectric layer (PTFE, FEP, Kapton, Nolyn) and two metal electrodes (Cu or Al). As shown from Fig. 4a to Fig. 4f [90–94], a basic structure with a single dielectric ball and two metal electrodes attaching on the outer shell is related to the inner structural characteristics of contact interface, rolling rate, freestanding height, electrode gap. The relative motion of rolling balls between dielectric layer and metal electrode from the triggering of HE-OWE can transform to the roll of ball in the shell at any direction, resulting in the transform 3D full-space mechanical

energy. During the process of rolling ball, contact electrification and electrostatic induction can be generated and subsequently alternative current flows through the external circuit with the charges yielded. It means that this type of S-TENG can harvest HE-OWE from any direction. If the direction of HE-OWE harvesting is determined, it can be achieved through adding the board. There shows the absolute advantages of infinite structural design and the flexibility of the structural design. The increasing size of rolling ball and the soft rolling ball being full of soft materials provide the possibilities of obtaining the excellent output performance due to increasing contact area. In the meantime, rolling rate of rolling ball and freestanding height are the representative of frequency and amplitude of HE-OWE under the triggering of HE-OWE. The electrode gap is inversely proportional to the output performance. In the meantime, these types of S-TENGs possess the merits of low cost, simple structure and easy to fabricate as well as demerit of poor durability owing to interfacial wear of rolling.

However, the space utilization of these types of S-TENGs are not taken into account, that is an important factor of improving the electrical output. As exhibited from Fig. 4g to Fig. 4m [95–101], contact interface and space utilization are the important impactors, in which it can be realized by decreasing the rolling ball size and increasing the number of balls, changing clearance and modifying electrode gap. The high charges outputs are provided under the condition of above. In order to inhibit the damage of contact interface, the novel inner structure of S-TENGs is proposed in Fig. 4n [102], which is composed of a pendulum and two Cu electrodes. In this way, the wear between dielectric layers and Cu electrode disappeared due to the separated distance between them and there only shows the electrostatic induction charges with the reciprocation of pendulum appears as the ocean wave moves back and forth. Subsequently, to yield the triboelectric charges by contact electrification along with the electrostatic induction, the method of fur is introduced, as shown in Fig. 4o [103]. However, despite the triboelectric charges and electrostatic induction charges are generated, output performance is limited resulting from the inadequate interface contact between fur and metal electrodes, producing finite triboelectric charges. In order to further improve the output performance along with the durability of S-TENGs, the other kinds of novel inner structure are proposed, including the non-contact, pendulum, Cu electrode induced by magnetic buoy, dielectric layer activated by water, the moment of inertia of the rotor or rolling metal balls, as illustrated from Fig. 4p to Fig. 4t [104–108]. It is noted that affecting factors can be summarized as the contact area, space utilization and frequency. In such case, the durability, stability and robust as well as effectiveness of S-TENGs can be absolutely improved. Multiple forms of energy such as sliding, vibration and rotation from the HE-OWE are suitable for harvesting for F-T-L working mode. Typical electric outputs characteristics from the conversion of the various forms of energy as described above contain high energy conversion efficiency, high short-circuit current, high output power and transferred charges, depending on the above structural characteristics.

As shown in Fig. 5, there exhibits the representative of harvesting HE-OWE for S-TENGs working in the C-S mode. There exhibit the inherent structural characteristics, such as vertical movement and a large separated clearance, and features of output performance, including high output voltage and high pulse. The vertical movement is expressed as the contact interface and contact-separation speed. And space utilization is not overlooked. In order to obtain the large fully contact interface, triboelectric thin film having inherent large area and excellent space utilization in the limited area are the better method. For example, the increasing contact-separation frequency Origami-inspired electret-based triboelectric generator is designed, as depicted in Fig. 5a [109]. In addition, the other assist methods, such as spring, heavy body, or assist body outside the shell, can be introduced to change contact interface, contact rate and separation clearance between the two. the assisted methods of the multilayered inner structure, such as the spring-assisted, ball-assisted, heavy balls, acrylic board and mass block ways, are

introduced to enhance the sensitiveness of S-TENG to ocean waves, boosting the increase of contact frequency, as shown from Fig. 5b to Fig. 5i [110–117]. Whirling-folded structure are introduced so as to increase the contact area in the limited space of oblate spherical structure, as shown in Fig. 5j [118]. Under the effect of these assisted methods, a faster process of compression and release are carried out with the back and forth of ocean waves and the contact-separation speed are enhanced. Moreover, the charge shuttling effect by the combination of several TENGs results in the significant improvement of electric output performance [119]. Besides to above, the introduction of spring can achieve the conversion from inputting low-frequency to outputting high-frequency HE-OWE. The heavy body can boost the occurrence of fully contact interface so as to convert HE-OWE to vibration or pressing forms of energy with large amplitude effectively. These kinds of S-TENGs can be applied to various occasions like vibration, pressing and impacting. However, the limited space inside S-TENGs requires the better space utilization. In a word, contact interface, contact frequency and space utilization have to be considered for these two working modes in inner structure of S-TENGs. The fundamental analysis should be commenced with the above three important factors.

3. Characterization of S-TENGs

Based on the fundamental working modes being divided, TENGs having various structure are designed and put it into the interior of hollow spherical shell. The S-TENGs is subjected to external forces generating from ocean waves having the arbitrary low-frequency at any direction and move back and forth periodically with the movement of ocean waves when S-TENGs float freely without any support on the ocean. However, there still not comprehensively and systemically demonstrates the common characterizations of all the S-TENGs from these three aspects, including inner structure, triboelectric materials and working modes.

3.1. Frequently-used triboelectric materials of S-TENGs

Fig. 6 depicts percentage of triboelectric polymer materials working in different working mode and solid-liquid materials used as triboelectric materials. One important consideration for S-TENGs is the choice of dielectric materials with high contact electrification charges, desired wearable resistance properties, and environmental friendliness and stability. We summarized the most commonly used triboelectric materials of S-TENGs in the past decades, including PTFE, FEP, Kapton, Nylon, etc. To date, there shows 52.4 % for the percentage of PTFE, 60 % for the percentage of FEP when S-TENGs work in the F-T-L mode and C-S mode, respectively, as shown in Fig. 6a and b. And there exhibits the low percentage of liquid used as triboelectric materials, 6.5 %, as shown in Fig. 6c. It has been proved that triboelectric charge density (TECD) exhibits the values of $-113.06 \mu\text{C}/\text{m}^2$, $-102.05 \mu\text{C}/\text{m}^2$, $-92.88 \mu\text{C}/\text{m}^2$, $-71.20 \mu\text{C}/\text{m}^2$, $-47.30 \mu\text{C}/\text{m}^2$, $-26.09 \mu\text{C}/\text{m}^2$, respectively, for the dielectric materials of PTFE, PDMS, Kapton, FEP, silicone, Nylon [120]. It indicates that PTFE possesses the higher TECD than FEP.

It is apparent that the polymer material surfaces with different functional groups can not only improve the charge density, but also change the polarity of its charge [121]. The functional group structure can be modified so as to generate strong electron-donating groups, greatly increasing the charge density of the electricity [122]. In addition, the polarity of charges is closely related to the electronegativity of dielectric materials. The electronegativity of PTFE is more excellent than FEP due to the presence of unsaturated groups on the molecular chain [123]. The higher electronegativity of dielectric materials is, the stronger inherent ability of obtaining the electron is. The excellent electric performance is obtained more easily. The order of the electronegativity from strong to weak is FEP, PTFE and PVDF. According to the TECD and electronegativity, PTFE and FEP are often used as the primary polymer materials of dielectric layer for F-T-L and C-S working mode. To

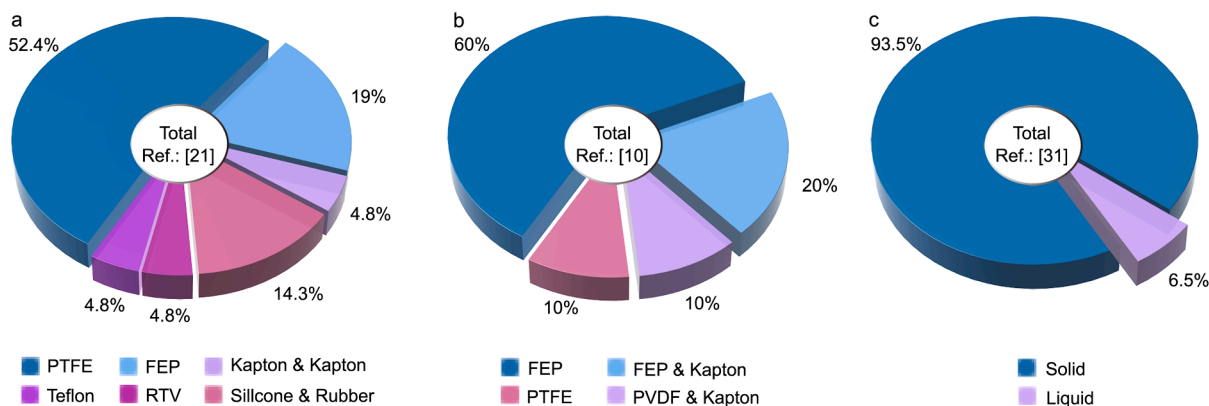


Fig. 6. Percentage of triboelectric polymer materials working in different working mode for S-TENG and solid-liquid materials used as triboelectric materials for S-TENG. (a) Percentage of different triboelectric polymer materials in F-T-L working mode for S-TENGs. (b) Percentage of different triboelectric polymer materials in C-S working mode for S-TENGs. (c) Percentage of solid and liquid triboelectric materials for S-TENGs.

obtain the high electronegativity of polymer materials, acquiring more surface unsaturated functional groups on PTFE ultra-thin film is a better way by ion irradiation [122], surface magnetron sputtering [123], 3D printing [124,125], surface plasma [126], etc. The other material's surface treating technologies, i.e., heating [127], polishing [128], or chemical modification [129,130], etc. are prevalent and have been utilized in numerous investigations to augment the output performance of TENGs with other exteriors, which these technologies are also applied in S-TENGs. However, the poor wearable resistance restricts the service life and excellent durability in the S-TENGs working in the F-T-L mode.

Thus, developing the new dielectric materials with the merits of large wearable resistance, high charge density, high electronegativity and low cost are essential.

On the other hand, FEP is another choice of triboelectric materials owing to the relative better wearable resistance, whereas higher cost than PTFE. FEP are more suitable for C-S working mode on the basis of the stronger ability of obtaining or losing the electron than PTFE during the contact-separation process due to a large amount of fluorine group, increasing the triboelectric charge density. Overall, enhancement of large TECD, strong electronegativity and high wearable resistance as

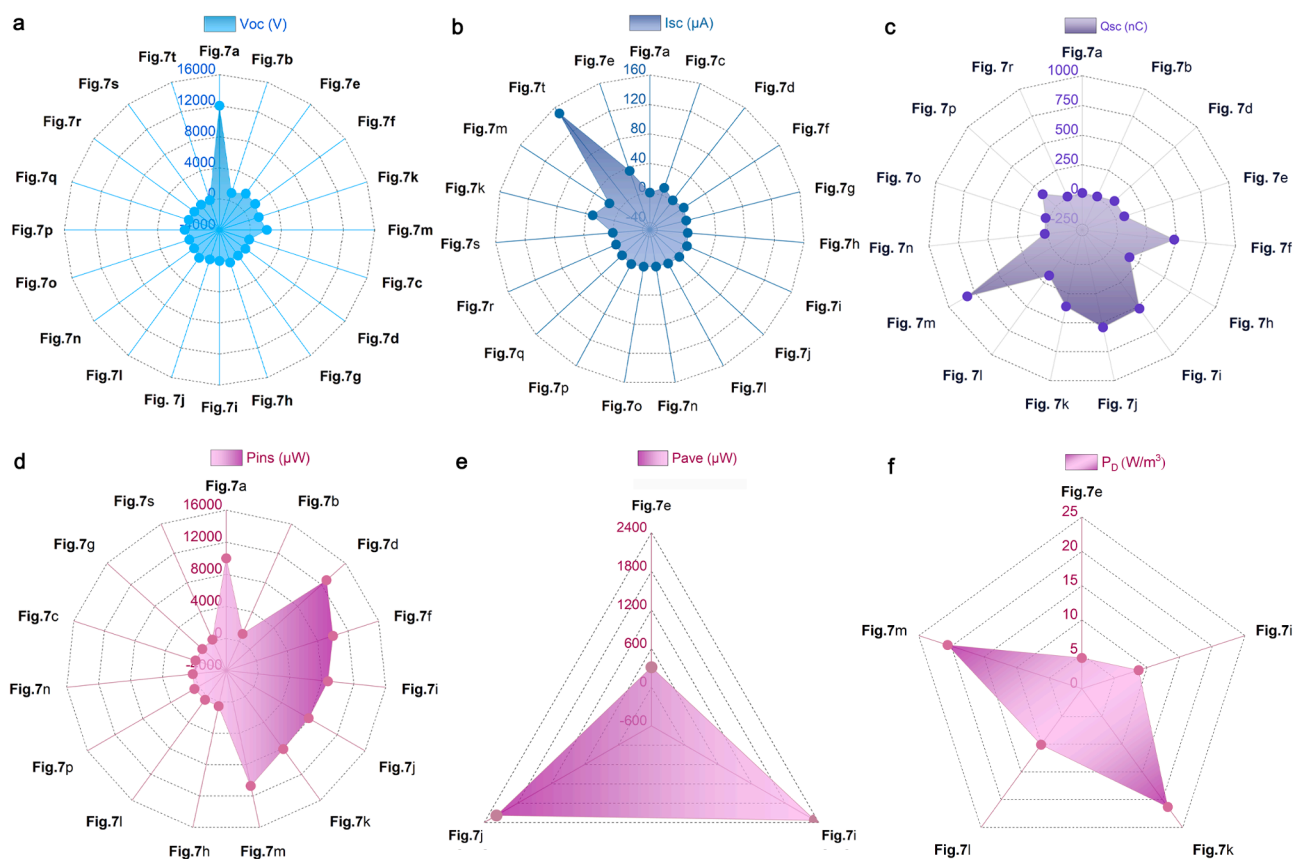


Fig. 7. Output performance of S-TENG with F-T-L working mode. (a) Open-circuit voltage (V_{oc} , V) of S-TENG. (b) Short-circuit current (I_{sc} , μA) of S-TENG. (c) Transferred charges (Q_{sc} , nC) of S-TENG. (d) Instantaneous power (P_{ins} , μW) of S-TENG. (e) Average power (P_{ave} , μW) of S-TENG. (f) Power density (P_D , W/m^3) of S-TENG.

well as low cost are inevitable trend toward seeking the new dielectric materials.

3.2. Electrical output performance of S-TENGs

Among the various forms of water wave energy harvesters, S-TENGs is the commonly used device through the results of Fig. 3b. It is considered that the S-TENGs possess the unique merits, such as infinite design space of inner structure, excellent output performance, simple structure, and integration easily, compared to the other forms of water wave energy harvesters. Generally speaking, the output electric performances of S-TENGs are important specifications, playing an important role in evaluating quality and commercial application. The electric outputs from free electrons flowing through the external circuit can be obtained with contact-separation movement or sliding movement of dielectric layer on one or two metal electrodes driven by water wave energy. The statistic results of output electric performances and corresponding structure of S-TENGs are summarized and analyzed, as shown in Fig. 7 and Fig. 8 as well as Table 1 and Table 2, in which the range of electric outputs of S-TENGs is composed of open-circuit voltage (V_{oc} , V), short-circuit current (I_{sc} , μA), instantaneous power (P_{ins} , μW), the instantaneous power density (P_D , W/m^3), the amounts of transferred charges (ΔQ_{sc} , nC) and average power (P_{ave} , μW), clearly showing that the electric outputs of S-TENGs have reached a fairly high level, such as maximum output performance of 12000 V, 1400 μA , 74000 μW , 2330 μW , 1700 nC, 27.8 W/m^3 , respectively [91,100,111,118]. As demonstrated above, F-T-L and C-S working modes are usually used in S-TENGs. Fundamentally speaking, discrepancy of output performance is intimately related to the multiform inner structure based on different working modes, multifarious materials and interface circuit.

There shows output performance of S-TENGs with F-T-L working mode in Fig. 7 and Table 1, corresponding to the inner structure in Fig. 4. In the case of similar amplitude and frequency of ocean waves as well as the same inner structure from Fig. 4a to c, the output performance, 12000 V and 1000 V, and 10000 μW and 1000 μW , exhibit the large difference while Kapton with nanowire structure on surface and PTFE are used as the triboelectric materials, respectively [91]. By contrast, the rolling ball-S-TENG in Fig. 4c exhibits the low voltage and small current, resulting from the main cause of pair of Au and PTFE [90]. It is concluded that the nanowire structure on surface act as the important role in obtaining the different output voltage and output power because of the remarkable increased contact interface, even if the triboelectric charge density for PTFE is higher than Kapton [91], whereas the combination of Al and Nylon serves as the major role in generating high voltage and large current. For this type of TENG, small current and the small amounts of transferred charges as well as the unstable output limits the applications severely. Subsequently, increasing contact area and contact continuously in a long time is the key way. With the increased contact interface by introducing the soft silicone rubber (Fig. 4e) and liquid (Fig. 4f), the output voltage, output current, instantaneous power and transferred charge is highly increased, which obtain the output current of 34.5 μA and transferred charge Q_{sc} of 480 nC. High instantaneous power P_{ins} of 12830 μW is yielded, which comprehensive performance is better than the other S-TENGs with a rolling ball [90–92]. Even though the TECD of silicone rubber is lower than the PTFE, electric output performance of S-TENGs using silicone rubber as triboelectric layers is better than the S-TENGs using PTFE by comparing with Fig. 4b and e and f. It is inferred that increasing the contact interface by using soft ball in S-TENG is a better method of improving output performance, especially the output transferred

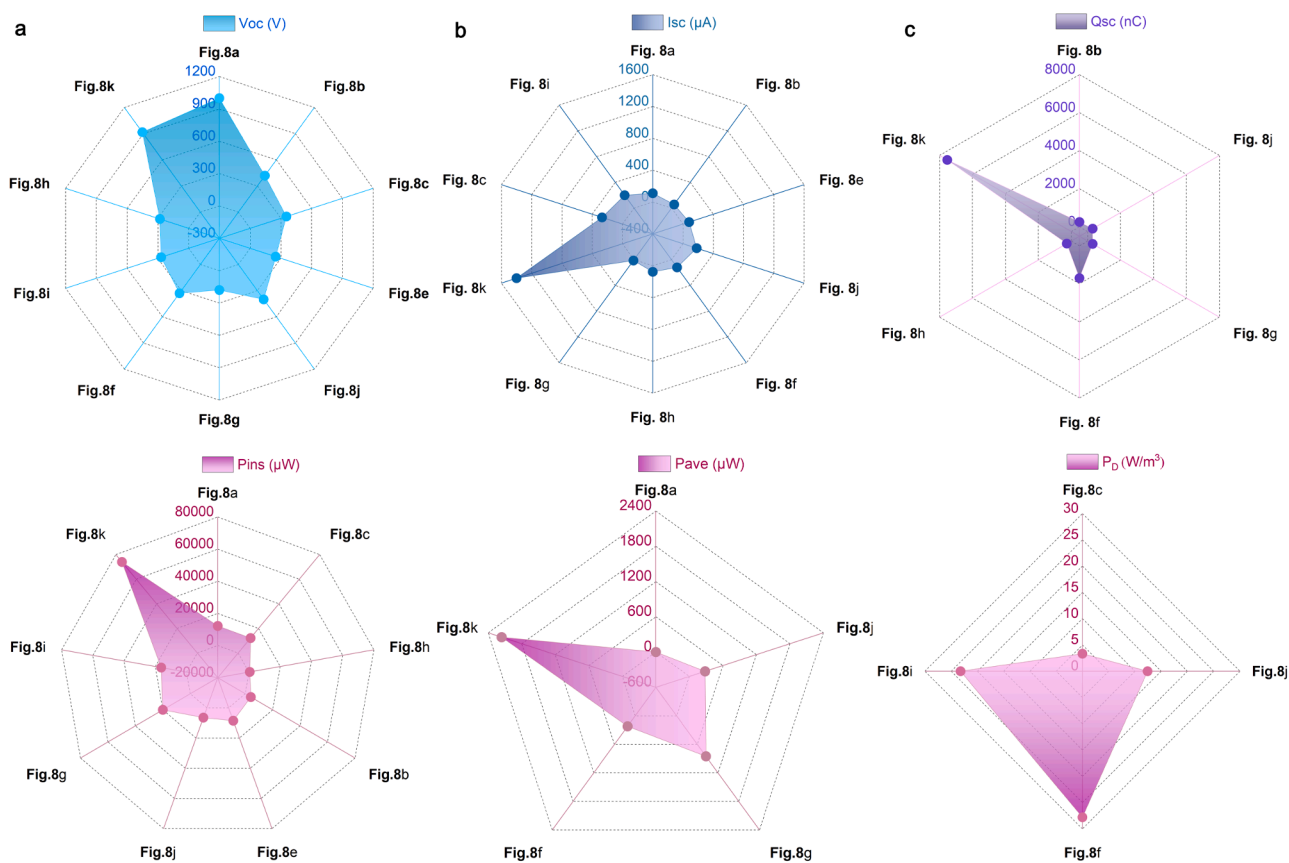


Fig. 8. Output performance of S-TENG with C-S working mode. (a) Open-circuit voltage (V_{oc} , V) of S-TENG. (b) Short-circuit current (I_{sc} , μA) of S-TENG. (c) Transferred charges (Q_{sc} , nC) of S-TENG. (d) Instantaneous power (P_{ins} , μW) of S-TENG. (e) Average power (P_{ave} , μW) of S-TENG. (f) Power density (P_D , W/m^3) of S-TENG.

Table 1
Summary and comparison of all kinds of S-TENGs with in F-T-L working mode.

| Figure | Ref. | Electrodes | Active materials | Structure | Output electric performance | Advantages | Disadvantages |
|---------|-------|------------|------------------|--|--|---|---|
| Fig. 7a | [91] | Al | Kapton & Nylon | A rolling ball structure | $V_{oc} = 12$ kV, $I_{sc} = 1.2$ μ A, $P_{ins} = 10000$ μ W, $Q_{sc} = 12$ nC. | High voltage, light weight, simple structure. | Low current, low transferred charge poor durability, poor output stability, low conversion efficiency. |
| Fig. 7b | [91] | Al | PTFE | A rolling ball structure | $V_{oc} = 1$ kV, $P_{ins} = 1000$ μ W, $Q_{sc} = 9$ nC. | High voltage, light weight, simple structure. | Low current, poor output stability, poor durability, low conversion efficiency. |
| Fig. 7c | [90] | Au | PTFE | A rolling ball structure | $V_{oc} = 31.7$ V, $I_{sc} = 10$ μ A, $V_{ins} = 34.5$ μ W. | Low cost, simple structure, easy to fabricate, stable electric output, good durability. | Poor output stability and durability, low conversion efficiency. |
| Fig. 7d | [92] | Cu | Teflon | A rolling ball structure | $V_{oc} = 139.46$ V, $I_{sc} = 0.66$ μ A, $Q_{sc} = 65.13$ nC. | Light weight, simple structure, easy to prepare, good output stability. | Low power, low current, poor retention efficiency, poor durability, low conversion efficiency. |
| Fig. 7e | [94] | Ag-Cu | Silicone Rubber | A soft rolling ball structure | $V_{oc} = 1.78$ kV, $I_{sc} = 34.5$ μ A, $P_{ins} = 12830$ μ W, $P_{ave} = 310$ μ W, $Q_{sc} = 72.6$ nC, $P_D = 4.47$ W/ m^3 . | Light weight, simple structure, high current, high responsivity. | Low transferred charge, low power density, poor output stability, poor durability, low conversion efficiency. |
| Fig. 7f | [93] | Cu | Silicone Rubber | A rolling ball structure | $V_{oc} = 1.7$ kV, $I_{sc} = 5$ μ A, $P_{ins} = 10000$ μ W, $Q_{sc} = 480$ nC. | Light weight, simple structure, high voltage, high current, easy to fabricate. | Poor durability, poor output stability, low conversion efficiency. |
| Fig. 7g | [99] | Cu | Magnet ball | triboelectric-electromagnetic hybrid structure | $V_{oc} = 88$ V, $I_{sc} = 0.95$ μ A, $P_{ins} = 18$ μ W. | Excellent space utilization, good output stability, simple structure and fabrication process. | Low current, poor durability, low conversion efficiency. |
| Fig. 7h | [101] | Cu | PTFE | Matryoshka-inspired hierarchically structure | $V_{oc} = 430$ V, $I_{sc} = 1.64$ μ A, $P_{ins} = 544$ μ W, $Q_{sc} = 160$ nC. | Light weight, low cost, high efficiency, excellent space utilization, good output stability. | Low current, low transferred charge, poor durability, low conversion efficiency. |
| Fig. 7i | [100] | Cu | FEP | Macroscopic encapsulated structure | $I_{sc} = 5$ μ A, $P_{ins} = 8750$ μ W, $P_{ave} = 2330$ μ W, $Q_{sc} = 520$ nC, $P_D = 8.69$ W/ m^3 . | Good durability, high power density, excellent space utilization. | Complex fabrication process, poor output stability, low voltage, low conversion efficiency. |
| Fig. 7j | [96] | Al | PTFE | a pair of multilayer electrodes structure | $V_{oc} = 2.5$ V, $I_{sc} = 4.34$ μ A, $P_{ins} = 7880$ μ W, $P_{ave} = 2180$ μ W, $Q_{sc} = 540$ nC. | Low cost, high power, good durability, high transferred charge. | Poor output stability, complex structure, low conversion efficiency. |
| Fig. 7k | [97] | Cu | PTFE | Multilayer beads structure | $V_{oc} = 1.335$ kV, $I_{sc} = 30$ μ A, $P_{ins} = 8100$ μ W, $Q_{sc} = 360$ nC, $P_D = 21.3$ W/ m^3 . | High voltage, excellent space utilization. | Poor durability, poor output stability, complex fabrication process, low conversion efficiency. |
| Fig. 7l | [95] | Cu | Silicone | Soft Ball-Based Triboelectric–Electromagnetic Hybrid structure | $V_{oc} = 450$ V, $I_{sc} = 2$ μ A, $P_{ins} = 500$ μ W, $Q_{sc} = 175$ nC, $P_D = 10.1$ W/ m^3 . | High voltage, increased contact area, simple structure, low cost. | Poor durability, poor output stability, low conversion efficiency. |
| Fig. 7m | [98] | Al | FEP | Dense Point Contacts structure | $V_{oc} = 72$ V, $I_{sc} = 15.5$ μ A, $P_{ins} = 10700$ μ W, $Q_{sc} = 820$ nC, $P_D = 20.57$ W/ m^3 . | High transferred charge, output stability, high power density, high voltage, excellent space utilization. | Poor durability, Complex fabrication process, low conversion efficiency. |
| Fig. 7n | [102] | Cu | PTFE | Pendulum structure | $V_{oc} = 55$ V, $I_{sc} = 0.6$ μ A, $P_{ins} = 195.6$ μ W, $Q_{sc} = 18.2$ nC. | Low cost, simple structure, easy to fabricate, stable electric output, good durability. | Low current, low conversion efficiency. |

(continued on next page)

Table 1 (continued)

| Figure | Ref. | Electrodes | Active materials | Structure | Output electric performance | Advantages | Disadvantages |
|---------|-------|------------|------------------|--|--|--|---|
| Fig. 7o | [38] | Cu | PTFE | Pendulum structure | $V_{oc} = 75.6 \text{ V}$, $I_{sc} = 0.74 \text{ } \mu\text{A}$, $Q_{sc} = 25 \text{ nC}$. | Excellent durability, stable voltage output, simple structure, low cost. | Low current, low power, low conversion efficiency. |
| Fig. 7p | [103] | Cu | PTFE | Gyroscope structure | $V_{oc} = 480 \text{ V}$, $I_{sc} = 3 \text{ } \mu\text{A}$, $P_{ins} = 600 \text{ } \mu\text{W}$, $Q_{sc} = 150 \text{ nC}$. | Good output stability, high voltage, low cost. | Complex structure, low conversion efficiency. |
| Fig. 7q | [107] | Cu | PTFE | Hybridized structure with multiple layer and magnetic ball | $V_{oc} = 172.95 \text{ V}$, $I_{sc} = 1.25 \text{ } \mu\text{A}$. | Low cost, simple structure, easy to fabricate, effective harvesting. | Low current, poor output stability, poor durability, low conversion efficiency. |
| Fig. 7r | [108] | Al | PTFE | Having water inside S-TENG | $V_{oc} = 15.2 \text{ V}$, $I_{sc} = 0.12 \text{ } \mu\text{A}$, $Q_{sc} = 8 \text{ nC}$. | Low cost, simple structure, easy to fabricate, output stability and robust, less susceptible to water leakage. | Poor durability, low conversion efficiency. |
| Fig. 7s | [106] | Al | FEP | Eccentric structure | $V_{oc} = 18.4 \text{ V}$, $I_{sc} = 0.49 \text{ } \mu\text{A}$, $P_{ins} = 230 \text{ } \mu\text{W}$. | Low cost, stable electric output, good robust and durability | Complex structure, hard to fabricate, low conversion efficiency. |
| Fig. 7t | [104] | Cr & Ag | FEP | angle-resolved structure | $V_{oc} = 38 \text{ V}$, $I_{sc} = 150 \text{ } \mu\text{A}$. | Simple method, energy-efficient, robust and low-cost, stable output voltage. | Low power, low conversion efficiency. |

Table 2

Summary and comparison of all kinds of S-TENGs with C-S working mode.

| Figure | Ref. | Electrode | Triboelectric materials | Structures | Electric output performance | Advantages | Disadvantages |
|---------|-------|-----------|-------------------------|--|---|--|---|
| Fig. 8a | [109] | Cu | FEP | Origami structure | $V_{oc} = 1 \text{ kV}$, $I_{sc} = 110 \text{ } \mu\text{A}$, $P_{ins} = 12200 \text{ } \mu\text{W}$, $P_D = 0.67 \text{ } \mu\text{W}$. | Simple structure, low cost, high voltage, good durability, high current. | Poor output stability, limited gap, low energy conversion efficiency. |
| Fig. 8b | [113] | Cu | FEP | Spring-assisted swing structure | $V_{oc} = 419 \text{ V}$, $I_{sc} = 56.7 \text{ } \mu\text{A}$, $P_{ins} = 4100 \text{ } \mu\text{W}$, $Q_{sc} = 250 \text{ nC}$. | Simple structure, low cost, high voltage, high power. | Poor output stability, poor durability, limited gap, low energy conversion efficiency. |
| Fig. 8c | [115] | Al | FEP | Spring-assisted multilayered structure | $V_{oc} = 354 \text{ V}$, $I_{sc} = 270 \text{ } \mu\text{A}$, $P_{ins} = 12200 \text{ } \mu\text{W}$, $P_D = 3.33 \text{ W/m}^3$. | High voltage, high current, low cost, simple structure, excellent space utilization. | Poor output stability, poor durability, limited gap, low energy conversion efficiency. |
| Fig. 8e | [114] | Cu | FEP | Spring-assisted multilayered structure | $V_{oc} = 250 \text{ V}$, $I_{sc} = 80 \text{ } \mu\text{A}$, $P_{ins} = 8500 \text{ } \mu\text{W}$. | High power, simple structure, excellent space utilization, output stability. | Low power density, limited gap, poor durability and output stability, low energy conversion efficiency. |
| Fig. 8f | [111] | Cu | Kapton & PVDF | Self-charge excitation multilayer structure | $V_{oc} = 330 \text{ V}$, $I_{sc} = 120 \text{ } \mu\text{A}$, $P_{ave} = 220 \text{ } \mu\text{W}$, $Q_{sc} = 1700 \text{ nC}$, $P_D = 27.8 \text{ W/m}^3$. | High transferred charge, high power, high power density. | Limited gap, poor durability and output stability, low energy conversion efficiency. |
| Fig. 8g | [112] | Al | PTFE | Nugget-assisted swing structure | $V_{oc} = 180 \text{ V}$, $I_{sc} = 12.5 \text{ } \mu\text{A}$, $P_{ins} = 20000 \text{ } \mu\text{W}$, $P_{ave} = 850 \text{ } \mu\text{W}$, $Q_{sc} = 300 \text{ nC}$. | High power, simple structure, high transferred charge, excellent space utilization. | Limited gap, poor durability, poor output stability, low energy conversion efficiency. |
| Fig. 8h | [118] | Cu | FEP | oblate spheroidal TENG assembled by two novel TENG parts | $V_{oc} = 281 \text{ V}$, $I_{sc} = 76 \text{ } \mu\text{A}$, $P_{ins} = 475 \text{ } \mu\text{W}$, $Q_{sc} = 270 \text{ nC}$. | Stable charge distribution, excellent space utilization, working in rough or halcyon seas, high response in small agitations, self-stabilization, and low consumables. | Harvesting horizontal motion energy, limited gap, poor durability, low energy conversion efficiency. |
| Fig. 8i | [110] | Cu | FEP | Multilayered structure | $V_{oc} = 268 \text{ V}$, $I_{sc} = 200.3 \text{ } \mu\text{A}$, $P_{ins} = 16200 \text{ } \mu\text{W}$, $P_D = 23.2 \text{ W/m}^3$. | High current, high power, high power density, excellent space utilization, stable output charge. | Limited gap, poor durability, low energy conversion efficiency, unstable output. |
| Fig. 8j | [116] | Cu | FEP | Whirling-folded structure | $V_{oc} = 400 \text{ V}$, $I_{sc} = 180 \text{ } \mu\text{A}$, $P_{ins} = 6500 \text{ } \mu\text{W}$, $P_{ave} = 280 \text{ } \mu\text{W}$, $Q_{sc} = 300 \text{ nC}$, $P_D = 12.4 \text{ W/m}^3$. | High power, simple structure, high current, excellent space utilization. | Limited gap, poor durability, poor output stability, low energy conversion efficiency. |
| Fig. 8k | [119] | Cu | PTFE | Charge-shuttling structure | $V_{oc} = 916 \text{ V}$, $I_{sc} = 1400 \text{ } \mu\text{A}$, $P_{ins} = 74000 \text{ } \mu\text{W}$, $P_{ave} = 2160 \text{ } \mu\text{W}$, $Q_{sc} = 7530 \text{ nC}$. | Ultrahigh projected charge density, excellent comprehensive performance. | Poor output stability, poor durability. |

charges. With soft-ball been more flexible, the more transferred charges are shown. Except for the above methods of nano interface and soft-ball, decreasing the size of rolling ball and enhancing the inner space utilization of sphere adquently can efficiently increase the contact area between rolling ball and metal electrode board, as shown from Fig. 4g to Fig. 4k. As shown in Fig. 4g and Table 1, output performance of 3D full-space triboelectric-electromagnetic hybrid nanogenerator is rather poor even with the help of EMG. And the issue concerning respective output of TENG and EMG is still not settled. Clearly, with the inner structure varied from the matryoshka-inspired hierarchically structure to condense points contact structure, there shows the improved trend for electric output performance, particularly the transferred charges, exhibiting the obvious increasing trend, such as 160 nC (Fig. 7h), 520 nC (Fig. 7i), 540 nC (Fig. 7j), 360 nC (Fig. 7k), 175 nC (Fig. 7l), 850 nC (Fig. 7k), indicating that the condense points contact structure to increase the amount of charges plays an important role. And it also shows the excellent instantaneous and average power and power density, which is 8750 μW (Fig. 7i), 2330 μW (Fig. 7i) and 21.3 W/m^3 (Fig. 7k), respectively, as shown in Table 1. Above all, increasing the number of rolling ball can efficiently increase the amount of transferred charges [98] and the split processing of rolling ball in the limited space can effectively improve the average power, that a small number of balls are placed into different grids [96]. As illustrated above, S-TENGs with the rolling ball can more easily obtain the probability of high voltage which is higher than 1000 V due to the specific dielectric materials of the pair of Nylon and Al [91].

Although the excellent output performance is obtained by designing the novel structure, particularly the condense points contact structure and selecting the suitable polymer materials, the existence of rolling friction led to the remarkable damage of contact interface, not facilitating the durability of electrical output. Thus, the other novel structure with the slight or even no wear are produced, such as pendulum structure, gyroscope structure via contact with the rabbit fur, sliding induced by magnet ball, water, eccentric structure, angle-resolved structure, corresponding to the results from Fig. 4n to Fig. 4s, electric output performance suffers a disastrous decline even though magnet induction and fur contact are presented, possibly resulting from the presence of electrostatic charges and the absence of the triboelectric charges. That is to say, the triboelectric charges have to be thus considered. In addition, despite the several rolling balls that is made of FEP polymer materials rolled on the Cr & Ag electrode board, the output performance is still lower than the forms of rolling ball and dense points contact due to the small contact interface and proper space utilization (Fig. 4t) [109]. That is suitable for driving the miniaturized electronic device. Overall, the complete filling of the internal space having the condense points contact structure exhibits the advantages of high transferred charge amount, high average power except for the high voltage, being conducive to obtain high-performance output based on F-T-L working mode. In which the large contact interface and/or proper space utilization are also not neglected. Furthermore, additional mechanisms and magnetic induction and decreasing the interfacial abrasion inspired by the oil could be used as the excellent approach of enhancing output performance and the durability. Meanwhile, there has to be widely applied in harvesting HE-OWE if the encapsulation technology is satisfied.

The output performance of S-TENGs working in C-S mode are depicted in Fig. 8 and Table 2, corresponding to the mainly used thin film structure in Fig. 5. The inner structural characteristics, including vertical movement and a large gap, can be as the representative of the large contact interface, contact-separation frequency, and space utilization. These are crucial factors for improving output performance obviously. Based on this, Origami-inspired structure, swing structure, spring-assisted thin film structure are designed and contact-separation movement induced by the external triggering is affected by the oscillator, spring and heavy copper ball, as shown from Fig. 5a to Fig. 5f. It is found that the output voltage, current and instantaneous power are improved together owing to the further increase of contact interface and

contact-separation frequency compared to the F-T-L working mode and, that are 1000 V, 120 μA , 8500 μW , 280 μW , 670 nC [112–117]. Particularly, the introduction of spring and mass block in the interior of contact separation S-TENG can convert the external low-frequency water wave motions to high frequency vibrations and the fully contact interface are achieved, improving the sensitiveness of external triggering and contact separation frequency on the basis of making full use of inner space. For example, the combination of heavy block and spring boosts the HE-OWE harvesting, that the instantaneous power attains up to 8500 μW . Besides the above, several TENGs with the multilayers structure in parallel and in series in the interior of S-TENGs facilitate the improvement of output performance, similar to the TENG-based network [112]. With heavy copper ball colliding with the acrylic substrates attached in the S-TENGs with vortex structure, the output instantaneous and average power reaches up to 6500 μW and 280 μW as well as volume power density of 12.4 W/m^3 under the triggering of water waves [116]. Moreover, the space utilization reaches 92.5 % for the multi-layer contact separation, such as 200.3 μA , 16200 μW (P_{ins}) and 23.2 W/m^3 (Fig. 5i) [110]. More importantly, combining the S-TENG having spring-assisted multilayered structure and power management module can achieve the multidirectional HE-OWE harvesting. Furthermore, with the PMM, the spherical TENG could output a steady direct current (DC) voltage on a resistance, and the charging speed to a supercapacitor was improved, that has been very close to the commercial application under the premise of excellent encapsulation.

In addition, the contact interface and contact-separation frequency can be changed by the other factors, such as suspension of the floating body. At present, the available energy conversion efficiency, the instantaneous output power, average power and transferred charge are up to 14.5 %, 20000 μW , 850 μW and 300 nC by the suspension of the floating body due to the interaction between liquid fluid and assist body in the water [112]. The increase of fully contact interface and contact-separation frequency by the assisted spring steel under the better space utilization can improve the comprehensive output performance for the oblate spheroidal TENG, such as 281 V, 76 μA , 475 μW and 270 nC [118]. Importantly, the oblate spheroidal shell has high response in small agitations, self-stabilization, and low consumables. And self-charge excitation achieves the charge injection on the surface of contact electrification, obtaining the average power of 220 μW and transferred charge of 1700 nC. (Fig. 5h) [111]. Generating the charge shuttling can be realized by using multiple TENGs in the interior of spherics jointly, as shown in Fig. 9, which charge injection from pump-TENG to main-TENG can improve the surface charge density efficiently and effectively under the help of huge contact area. And can enhance space utilization. It is excited that the comprehensive output performances are extremely high, that are 916 V, 1400 μA , 74000 μW , 2160 μW and 412 nC resulting from the charge shuttling effect through several TENGs in parallel [119]. For S-TENG with multi-layer contact separation structure under the help of combining with spring and joint use of multiple TENG, including the method of pump- and main-TENG and self-charge excitation, it is the best choice compared to the other types of TENGs and recommended to apply in real ocean environment if the issues on encapsulation technology and inhibiting the growth of microorganism are settled perfectly.

The S-TENG-based networks have been demonstrated to be an effective approach toward harvesting HE-OWE massively, that electric output of The S-TENG-based networks and corresponding structure of S-TENGs as shown in Fig. 10 and Table 3, compared to single S-TENG illustrated above. S-TENG-based network is connected in the forms of flexible or rigid connecting. For example, several S-TENGs connecting in parallel is a usual connecting way to improve the output current for C-S working mode as well as transferred charges and output power for F-T-L working mode. Apparently, advantages of extensive application occasion, stable performance output, quick charge and high voltage are shown using S-TENG-based network, as shown in Fig. 10 and Table 3. Output instantaneous and average power, and transferred charges

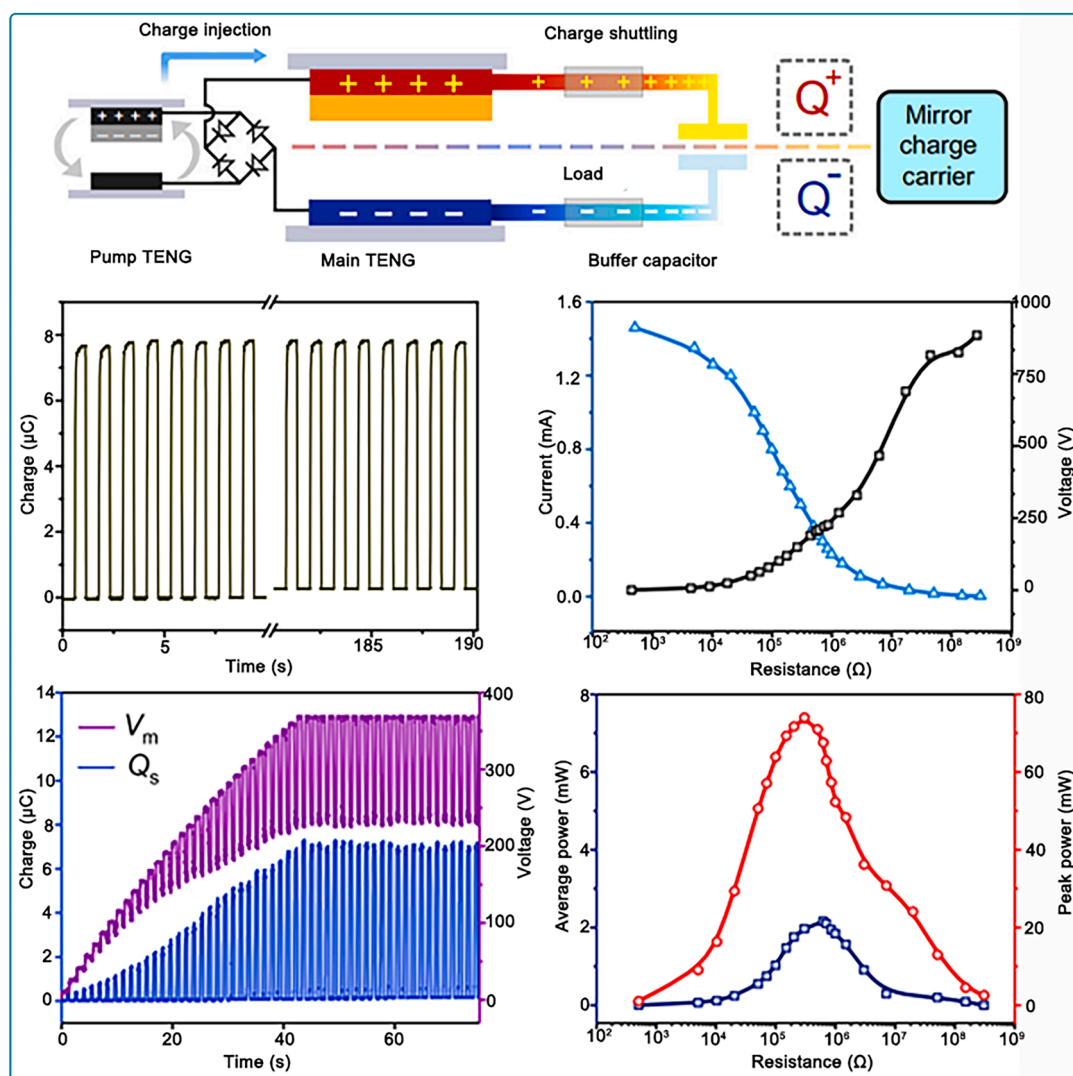


Fig. 9. Output performance of S-TENG with charge shuttling structure. It includes the work mechanism of S-TENG with charge shuttling structure, charges, current, voltage, peak power and average power. Reproduced with permission. [119] Copyright 2020, Springer Nature.

increased significantly, which is higher than 5 times compared to the single S-TENG unit. i.e., the maximum output power reaches 12 W [92], as well as the average power and transferred charges are 2.04 mW and 2138 nC, respectively, which is obviously larger than single S-TENG unit, 0.31 mW and 72.6 nC [94], the instantaneous power of 34.6 mW, average power of 9.89 mW and the transferred charges of 4900 nC are fairly higher than the corresponding single S-TENG unit, such as 8.75 mW, 2.33 mW, 520 nC [100]. S-TENG-based network connecting in series are inclined to generate high voltage as the S-TENGs work in C-S mode, which is in the range of 300–600 V. There shows the improved output performance for flexible connection of S-TENG-based network. And the improved output performance benefited from decreasing size of S-TENG unit and the increased number of S-TENG units. Moreover, the network covers a water area and extends into depth of water with each unit diameter, the high average power is expected to be delivered. In a word, S-TENG-based network acts a key role in improving the instantaneous power, average power and transferred charges.

In which energy conversion efficiency is a key parameter of expressing specific value of the output available energy and all input energy, which is expressed as

$$\eta = \frac{E_{avi}}{E_{all}}$$

where η is energy conversion efficiency, E_{avi} is output available energy and E_{all} is all input energy. It is well-known that introduction of spring facilitates the energy conversion efficiency to be enhanced largely owing to the increase of contact separation frequency. In addition, Zhang et al. [112] proposed an inverted pendulum-typed multilayer TENG to harvest HE-OWE in the wave height of 2–13 cm and wave frequency of 0.5–1.25 Hz. As shown in Fig. 8g, the proper mass of floating body increase efficiently contact area with the sea, enhancing the sensitiveness of S-TENGs to the wave. Contact separation frequency is thus increased and further the energy conversion efficiency is improved. Improving the energy conversion efficiency should be considered from the perspective of rising contact separation frequency for C-S working mode. For F-T-L working mode, it can be obtained by increasing sliding frequency. Thereby, introduction of spring in C-S mode and decreasing the wear in F-T-L mode is the main approach of enhancing energy conversion efficiency. This fundamental concept should be complied to design the novel inner structure of S-TENG.

In summary, the discrepancy of output performance of S-TENGs can be obtained by designing a diversity of inner structure, selecting different kinds of polymer materials having high TECD and strong electronegativity. Changing the inner structural characteristics include the fully contact interface, contact-separation frequency and better

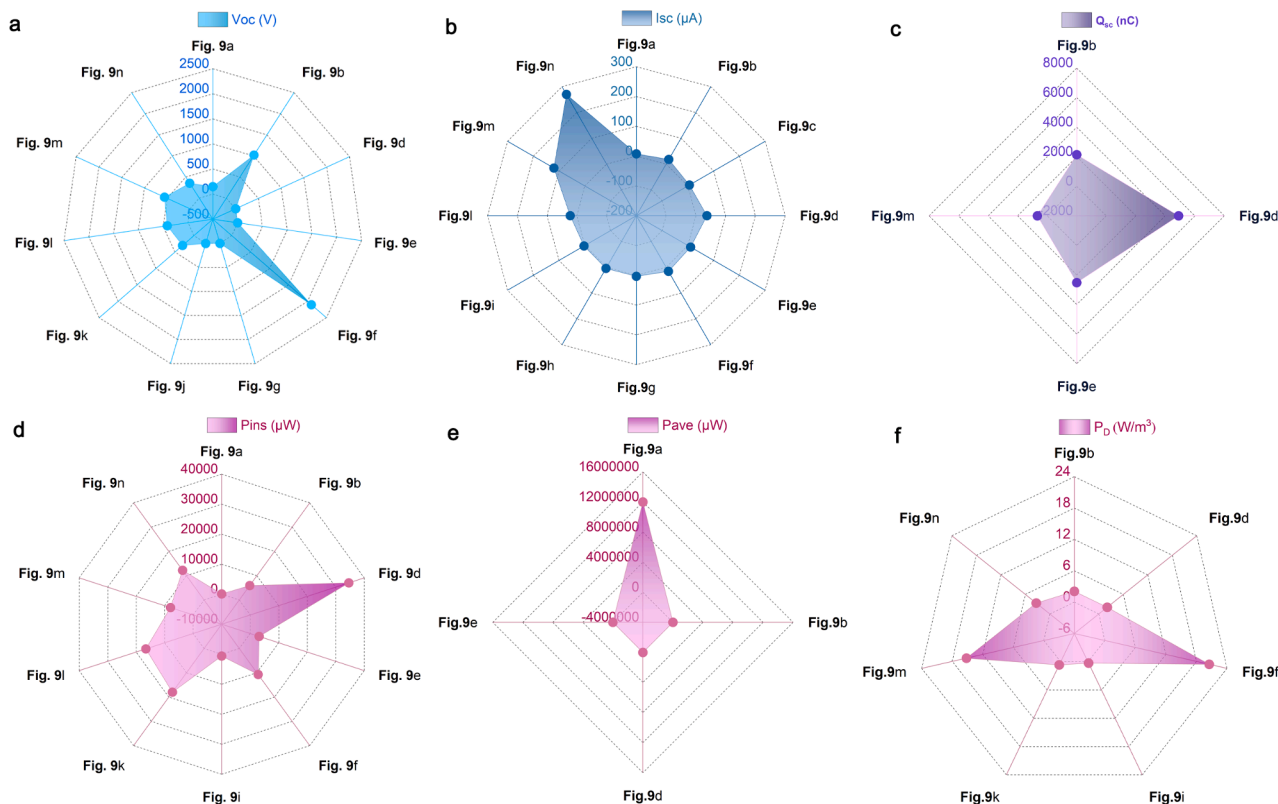


Fig. 10. Output performance of S-TENG-based network. (a) Open-circuit voltage (V_{oc} , V) of S-TENG. (b) Short-circuit current (I_{sc} , μA) of S-TENG. (c) Transferred charges (Q_{sc} , nC) of S-TENG. (d) Instantaneous power (P_{ins} , μW) of S-TENG. (e) Average power (P_{ave} , μW) of S-TENG. (f) Power density (P_D , W/m^3) of S-TENG.

space utilization as well as the movement velocity whatever the F-T-L and C-S working modes are. In addition, TECD is critical to TENG performance. Material surface modification for polymer materials that are commonly used as triboelectric layers and proper fabricating method are highly desired. And the relative work of searching for the new triboelectric materials, having the large TECD, strong electronegativity, high wearable resistance and low cost, cannot be terminated. Besides, the effects of affecting factors on the S-TENG-based network have been always carried out, including connection forms in parallel or in series, flexible or rigid connecting, the size of S-TENG unit, the number of S-TENG units. Moreover, the results that the principle of designing the network based on network applicability in severe marine environment, mechanism of improving performance for flexible connections are still not discussed in detail. However, the external environmental factors should be taken into account, i.e., specialized power management and energy storage circuits, external temperature and humidity, amplitude and frequency of ocean waves, etc. Therefore, specific S-TENGs with unique inner structure and dielectric materials can be applied in a certain application occasion in terms of output performance characteristics. So that, it is really difficult or even impossible thorough to distinguish good or bad output performance for different S-TENGs. Unfortunately, there are still lack of knowledge of these aspects.

3.3. Interface circuit

Except for above, interface circuit plays an important role. As illustrated above, the electric output should be the short AC pulse for most S-TENGs. Thus, it is essential for converting the AC to DC and store it before driving the electronic device. During this process, interface circuit acts as a key role [114,115]. The principle of interface circuit is based on low energy loss during the switching process, enhancing the output frequency, improving the output performance, DC output

through the interface circuit along with integrating with the S-TENGs more easily. Recently, much of work has been done to complete these ideas by designing the innovative interface circuit. An interface circuit for the TENGs that is transformerless and easily integrated, that is composed of large-capacity electrolytic capacitors and control section, containing the charging chip, rectifying circuit, a comparator chip and switch chip [131]. Su et al. proposed a novel self-powered interface circuit utilizing a dual-output rectifier for TENGs with C-S working mode. This circuit effectively rectifies the output into two distinct voltage magnitudes, specifically optimized for energy harvesting and self-powered switching generation, even under low-frequency and low-load conditions [132]. Hu et al [133] demonstrated an adaptable interface conditioning circuit, consisting of an impedance matching circuit, a synchronous rectifier bridge, a control circuit, and an energy storage device. Especially, the increase of frequency was achieved by a novel bi-directional switch control mechanism, reducing the energy loss of coupling inductance and increasing the output efficiency of TENG. In order to eliminate the energy loss, the circuit for AC to DC buck synchronous rectifier circuit is proposed [132]. For S-TENGs, it adopted the traditional interface circuit, including four diodes, switch, capacitor and load, leading to the disadvantages of huge energy loss, low output frequency and low output performance. More importantly, toward modular integration of the S-TENGs and the interface circuit and further miniaturized electronic devices are the trend in the future commercial application. However, it has many difficulties to be conquered, such as interface standardization, integration with chip and sensors, and so on.

3.4. Applicable scenarios

Development of wave energy is an important project that exploits the marine economy, including hydrogen production, artificial intelligence, fishery, desalination plant, etc. However, many of indeterminate factors

Table 3
Summary and comparison of S-TENG-based network.

| Figure | Ref. | Connecting mode | Output electric performance | Advantages | Disadvantages |
|----------|-------|-----------------|--|--|---|
| Fig. 10a | [94] | In parallel | $V_{oc} = 150$ V, $I_{sc} = 7.6$ μ A, $P_{ins} = 80$ μ W, $P_{ave} = 12$ W. | Stable output through rectifier, low cost, extensive application occasion, high average power, quick charge. | The principle of designing the network, poor applicability of network. |
| Fig. 10b | [93] | In parallel | $V_{oc} = 1020$ V, $I_{sc} = 18.1$ μ A, $P_{ins} = 5930$ μ W, $P_{ave} = 2040$ μ W, $Q_{sc} = 2138$ nC, $P_D = 2.06$ W/m ³ . | Stable output through rectifier, low cost, extensive application occasion, avoiding the drift of baseline, quick charge, high power, high current. | Relationship among covered area, each unit, water depth and maximum average power, principle of designing the network, poor applicability of network. |
| Fig. 10c | [100] | In parallel | $I_{sc} = 5.9$ μ A. | Stable output through rectifier, low cost, extensive application occasion, quick charge. | The principle of designing the network, poor applicability of network. |
| Fig. 10d | [96] | In parallel | $V_{oc} = 3.5$ V, $I_{sc} = 37$ μ A, $P_{ins} = 34600$ μ W, $P_{ave} = 9890$ μ W, $Q_{sc} = 4900$ nC, $P_D = 2.05$ W/m ³ . | Stable output through rectifier, low cost, extensive application occasion, high current, high power, quick charge. | The principle of designing the network, poor applicability of network. |
| Fig. 10e | [97] | In parallel | $V_{oc} = 1.75$ V, $I_{sc} = 10.69$ μ A, $P_{ins} = 3140$ μ W, $P_{ave} = 820$ μ W, $Q_{sc} = 2520$ nC. | Stable output through rectifier, low cost, extensive application occasion, be more adaptive to severe ocean environment. | Improving the applicability of network, furthermore improving the output performance. |
| Fig. 10f | [102] | In parallel | $V_{oc} = 2103$ V, $I_{sc} = 15.5$ μ A, $P_{ins} = 10700$ μ W, $Q_{sc} = 820$ nC, $P_D = 20.5$ W/m ³ . | Stable output through rectifier, low cost, extensive application occasion, quick charge, high voltage. | The principle of designing the network, poor applicability of network. |
| Fig. 10g | [103] | In parallel | $V_{oc} = 4.5$ V, $I_{sc} = 3.4$ μ A. | Stable output through rectifier, low cost, extensive application occasion, quick charge. | The principle of designing the network, poor applicability of network. |
| Fig. 10h | [105] | In parallel | $I_{sc} = 4.4$ μ A. | Stable output through rectifier, low cost, extensive application occasion, quick charge. | The principle of designing the network, poor applicability of network. |
| Fig. 10i | [107] | In parallel | $I_{sc} = 3.2$ μ A, $P_{ins} = 600$ μ W, $P_D = 0.28$ W/m ³ . | Stable output through rectifier, low cost, extensive application occasion, quick charge. | The principle of designing the network, poor applicability of network. |
| Fig. 10j | [106] | In parallel | $V_{oc} = 5.013$ V. | Stable output through rectifier, low cost, extensive application occasion, quick charge. | The principle of designing the network, poor applicability of network. |
| Fig. 10k | [109] | In series | $V_{oc} = 300$ V, $P_{ins} = 18000$ μ W, $P_D = 0.67$ W/m ³ . | Low cost, extensive application occasion, quick charge, long-term durability and excellent flexibility, high power. | Unstable output, the principle of designing the network, poor applicability of network. |
| Fig. 10l | [113] | In parallel | $V_{oc} = 419$ V, $I_{sc} = 22.3$ μ A, $P_{ins} = 16600$ μ W. | Stable output through rectifier, low cost, extensive application occasion, quick charge, high performance. | The principle of designing the network, poor applicability of network. |
| Fig. 10m | [117] | In parallel | $V_{oc} = 560$ V, $I_{sc} = 120$ μ A, $P_{ins} = 7960$ μ W, $Q_{sc} = 670$ nC, $P_D = 15.2$ W/m ³ . | Low cost, extensive application occasion, quick charge, high performance. | Unstable output, the principle of designing the network, poor applicability of network. |
| Fig. 10n | [115] | In series | $V_{oc} = 354$ V, $I_{sc} = 270$ μ A, $P_{ins} = 12200$ μ W, $P_D = 3.33$ W/m ³ . | Stable output through rectifier, low cost, extensive application occasion, quick charge, high performance. | The principle of designing the network, poor applicability of network. |

in ocean severely impede the exploitation of marine resources, in which power supply of marine device has been the main issue that cannot be thoroughly settled by the traditional technology. TENG acts as the better role in this aspect, in which application of S-TENG in harvesting HE-OWE is the best choice.

3.4.1. Harsh marine environment

Marine environment refers to the vast and continuous water area of ocean on the earth, including seawater, materials dissolved and floating in the ocean, sea sediments and marine life as well as microorganism, particularly the materials dissolved in the ocean and microorganism relying on the S-TENG. The materials dissolved in the ocean is composed of mainly chlorides, followed by sulfate. The salt content of seawater is usually expressed by salinity, that the salinity attains up to about 35 %, including sodium ions and chloride ions, serving as the main role in corroding the devices for electrolyte. Due to the existence of metal electrode, anti-corrosion is essential. In order to avoid the seawater

corrosion, selecting the anti-corrosion materials having insulating property and great encapsulation technology is an efficient and effective way to construct the anti-corrosion system. There shows the outstanding capability of anti-corrosion for some organic materials, including polyimide (PI), polytetrafluoroethylene (PTFE) and acrylic board, considering as the primary of shell. Subsequently, excellent encapsulation technology acts as an important role, such as sealed with epoxy paint. And material processing by alkaline treatment is also a feasible approach. Or developing the new electrochemical corrosion protection system is viable using the seawater in future. It is seen that the encapsulation technology is not suitable for the application in a large scale. In addition, the diverse microorganism in ocean, such as eukaryotic microorganisms (fungi, algae, and protozoa), prokaryotic microorganisms (marine bacteria, marine actinomycetes, and marine cyanobacteria, etc.), and cell-free organisms (viruses), is the other key factor of affecting the service life. Disrupt the growth conditions and preventing the growth of microorganisms can directly reduce the number of

microorganism on the surface of S-TENGs. The microorganism grows in the condition of nutrient-rich environments. So creating the nutrient-poor environment is essential by controlling the emission of phosphorus and nitrogen, changing the cycles of nitrogen. Where the nitrogen cycle can be achieved by the method of nitrogen fixation, nitrification, denitrification and anammox. In addition, reducing the concentration of CO₂ over the ocean by greening the vegetation of the land around the ocean can attain the reduction of carbon content in ocean and the elimination of the content of CO₂ entering into the ocean. By the above approach, the grow conditions of microorganism are disrupted, high-density array integration.

4. Current and potential applicable scenarios of S-TENGs

The focus of this section will demonstrate the current and potential applicable scenarios, as illustrated in Fig. 11. To date, S-TENGs are mainly applied in two aspects, including harvesting HE-OWE and self-powered sensing. A great deal of S-TENGs can assemble the networks to harvest the low-frequency HE-OWE in a large-scale, converting it into electric energy.

4.1. Current applicable scenarios

As illustrated above, the absolute advantages of S-TENGs is shown. Energy storage devices, including batteries and supercapacitors, not only provide the power source for other electronics by storing energy, but also play a key role in balancing energy supply and demand for integrated circuits. The electronic device around or in the sea can be driven by these types of power source by converting the HE-OWE harvesting from ocean into electronic energy. Until up to now, many of electronic devices are powered, such as LED device, intelligent wireless alarm system, humidity and temperature sensors, electric double-layer capacitors, thermometer, as shown from Fig. 11b to d and Fig. 11f, when the voltage is below the value of 10 V. It can be widely applied in ocean development. It is found that the commercial application in a large-scale is in fancy.

4.2. Potential applicable scenarios

4.2.1. Large-scale ocean energy power plant

The large-scale ocean energy power plant will be formed with the S-TENG array deployed in ocean, as shown in Fig. 11. The each unit in S-TENG network moves along any direction as the ocean waves hit S-TENG unit repeatedly and then electronic energies is yielded. The stable electric output can provide the power source of a long time for the coastal cities, platform on the ocean. In particular, the capability to harvest HE-OWE from any direction makes it as an ideal devices generating power. Compared to the traditional electric power generation, it has the advantages of low-cost and easy to maintain. In future, the research work should be focused on the integration and the modulus design to realize this great dream. By this way, the sufficient stability and reliability are ensured as the deployment of S-TENG-based network is being carried out. Meanwhile, the used materials and structure could be optimized by various method to improve the energy conversion efficiency, boosting the actual application of ocean energy power plant in a large-scale.

4.2.2. Power supply for aquaculture facilities of offshore fishery

Toward the developing trend of automation and intelligence is inevitable and electric supply is indispensable. A device for feeding fishes and environmental monitoring as well as communication system are powered by harvesting HE-OWE mounted on the platform or fishing cage. In this way, it can either reduce the dependence on external power supply, but also reduce the operating costs of fishery facilities. Importantly, the stable power supply has to be done, that can be achieved by harvesting the multi-dimensional energy from the motion and

harvesting HE-OWE in wide range of wave frequency by designing special switch. In the future, spherical TENG is expected to become an indispensable part of intelligent fishery aquaculture, contributing to the sustainable development of fishery.

4.2.3. Wave-driven navigation buoy

Marine navigation buoys play an important role in ocean navigation and traffic management. However, the issues concerning the maintenance in routine and replace the batteries result in the limitation of power supply. These navigation buoys could achieve the stable operation in a long time by self-powered approach using S-TENGs, reducing the cost of maintenance in routine. The combination of S-TENGs and intelligent buoys system will sustain the more advanced navigation, such as the real-time marine data transmission, ship positioning and tracking, promoting the development of intelligent marine traffic. The long-term stable power supply provided by S-TENG will significantly enhance the reliability of the navigation buoys system, especially the remote ocean.

4.2.4. Integration with the other marine device

It is found that hybrid energy system can be formed by integrating the S-TENGs with other existing ocean energy devices (such as tidal energy, solar energy), achieving the dream of intelligent electronic device [134]. In this way, the efficiency to harvest HE-OWE are largely improved by designing integrated modules, fostering the energy harvesting toward the diversification and stability. For instance, the additional electrical output of S-TENGs can be regarded as the supplement traditional electrical output as the ocean environment is in the low frequency and low amplitude. Hereafter, there will exhibit the ocean energy system having the characteristics of reliability and effectiveness through the approach of integrating with the other kinds of ocean energy devices.

4.2.5. Marine environmental monitoring

Marine environmental monitoring includes temperature, humidity, in-situ water quality, in-situ water level, commercial thermometers, climate prediction and marine disaster warning, that transmit the relative data through wireless communicative devices [135,136], the power supply is provided by HE-OWE harvested by S-TENGs. In the complex and changeable ocean, the power supply is often damaged and the marine devices are thus not worked. It is excited that the stable and continuous operation of marine environmental monitoring devices cannot be disrupted because the continuous work of S-TENGs while the waves and wind change dramatically. S-TENG can be deployed in global ocean warning networks, especially in coastal areas where disasters are high in the future. The development of S-TENGs will significantly improve the capability of marine disaster warning, eliminating the impact on human society.

Besides above, there shows the more application occasions in future, such as self-powered angle-resolved S-TENG in underwater environment, corrosion inhibition, air purification, seawater purification, high-voltage transmission [137] and internet of things (IoT) [138]. Based on internal factors, including inner structural characteristics and selective materials, and external impacting factors, such as power management circuit [139,140], energy storage technology [141–143], etc., we can obtain the proper output performance according to the specific application occasions. Nevertheless, the applications of S-TENG in HE-OWE harvesting and self-powered sensing are still at the initial stage. To this end, more explorations are highly desired to select the proper polymer materials, optimize the inner structure and performance of S-TENGs toward specific application occasions.

5. Conclusion and perspectives

As a new nanotechnology, S-TENGs have shown strong vitality and enormous advantage of applying in HE-OWE harvesting and self-

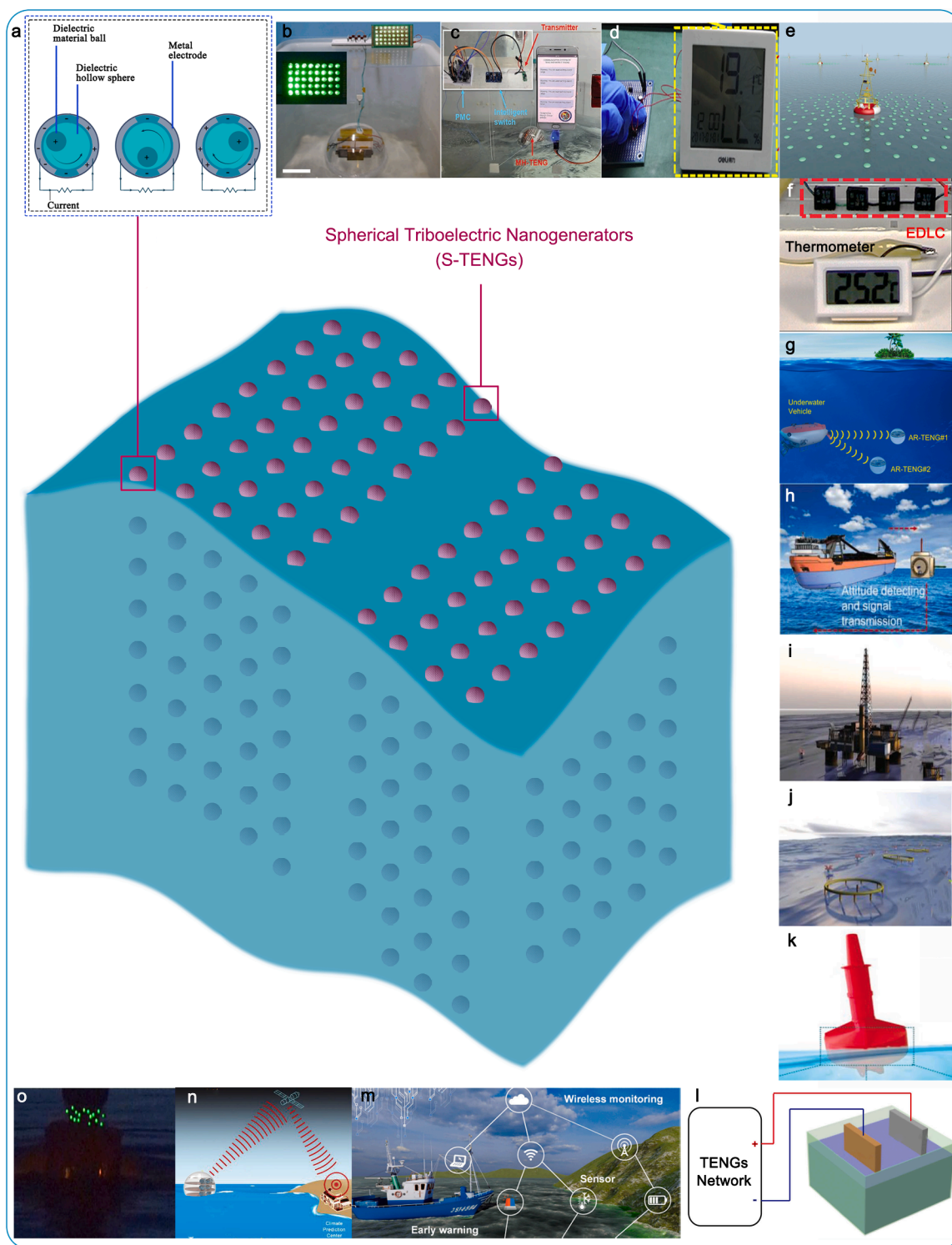


Fig. 11. Potential application occasions for S-TENG. (a) Working diagram of S-TENG. (b) Power source of LED. (c) Intelligent wireless alarm system. (d) Humidity and temperature sensors. (e) Buoy floating on the ocean. (f) Electric double-layer capacitors and thermometer. (g) Self-powered angle-resolved S-TENG in underwater environment. (h) Attitude detecting and signal transmission in navigation. (i) Platform on the ocean. (j) Fishery production. (k) Buoy. (l) Corrosion inhibition. (m) Self-powered environmental wireless monitoring. (n) Climate prediction center. (o) Self-powered alarm system of swimwear. (a) Reproduced with permission. [40] Copyright 2017, Springer Nature. (b) Reproduced with permission. [93] Copyright 2019, Elsevier. (c) Reproduced with permission. [110] Copyright 2023, Wiley-VCH. (d) Reproduced with permission. [99] Copyright 2020, Elsevier. (e) Reproduced with permission. [118] Copyright 2019, Wiley-VCH. (f) Reproduced with permission. [91] Copyright 2015, Wiley-VCH. (g) Reproduced with permission. [104] Copyright 2023, Elsevier. (h) Reproduced with permission. [51] Copyright 2017, Elsevier. (i) Reproduced with permission. [52] Copyright 2022, Wiley-VCH. (j) Reproduced with permission. [48] Copyright 2024, Elsevier. (k) Reproduced with permission. [65] Copyright 2021, Elsevier. (l) Reproduced with permission. [149] Copyright 2020, American Institute Physics. (m) Reproduced with permission. [45] Copyright 2023, Elsevier. (n) Reproduced with permission. [22] Copyright 2023, Wiley-VCH. (o) Reproduced with permission. [26] Copyright 2014, Elsevier.

powered sensing, which have great application prospects in HE-OWE. In order to make an overall grasp about S-TENGs, the current research progress is summarized in detail. With S-TENGs and S-TENG-based network provided the device for harvesting HE-OWE in a large-scale and application of ocean-related functional electronics, it is necessary to conduct a brief introduction of S-TENG and S-TENG-based network on a comprehensive investigation and detailed discussion on the internal relationship of single S-TENG among fundamental working modes, inner structural design, materials selection, interface circuit and output performance as well as present and future respective applicable scenarios. The results from above indicate that F-T-L and C-S working modes are commonly used in S-TENGs in terms of electric output features and structural characteristics. The irregularity and arbitrary on frequency and direction of ocean waves endows inner structure of S-TENGs with more design possibilities and diversified structure characteristics. Particularly, a large amount of recent research work on the relative structural characteristics, i.e., contact interface, contact frequency and space utilization as well as separation distance and gap, have been overviewed and corresponding discussions are also given. There exhibits the standard of materials selection, including high electronegativity, low cost, low friction coefficient and not easy to damage. For the different inner structure of S-TENGs and various materials selection, it can obtain the proper output performance for special application occasions. It is thus impossible to determine the good or bad output performance.

It is well-known that the reserves of HE-OWE are endless and there are several representative characteristics, i.e., sustainable, renewable and clean energy source, that are particularly noteworthy to achieve the marine application using S-TENGs. In which the important application are mainly two representative aspects such as HE-OWE harvesting and self-powered sensing. The potential applications of S-TENGs based on these two aspects are illustrated as follows:

- (1) *HE-OWE harvesting*: HE-OWE has the advantages of low-frequency (<5 Hz), irregularity, arbitrary direction and, in which S-TENGs are regarded as the most effective technology for all TENGs with various exterior due to its unique advantages such as infinite structural design, simple structure, integration easily, broader application, outstanding technology. S-TENGs enables to harvest HE-OWE efficiently in a multi-dimensional motion environment, providing a feasible power source supply for electronic device in or around the ocean such as the navigation floating buoy, marine electronic device, offshore fishery, integrating with other marine devices. It is firmly believed that S-TENGs will be bound to shine brightly in future HE-OWE harvesting.
- (2) *Self-powered sensing*: self-powered sensing is sensors of external information that is being measured without supplying the external power source. Then the measured external information is transformed to the electric signal. The development of HE-OWE and application of S-TENGs will contribute to the advancement of self-powered sensors in or around the marine environments, providing feasible implementation approaches, such as marine environmental monitoring, self-powered floating buoy and integrating with the other marine devices. In future, self-powered sensors have become an essential part of the information society which is reshaping our cognition.

In future, the relative researchers should concentrate on these aspects to further boost the commercial application, such as integrating the S-TENG and interface circuit, elongating the operation time after one triggering, enhancing motion frequency, increasing the contact area, improving encapsulation technology, eliminating the interfacial wear and increasing the charge transfer amount, and so on. Through the above approach, the commercial process will be accelerated due to the stable and proper output, long service life, more adaptable to harsh ocean environment. Even though great achievements being related to harvest the HE-OWE and self-powered sensing using S-TENGs have been

achieved according to theoretical research and multifaceted application demonstrations, there is still a huge gap between current research and practical commercial applications. Herein, potential difficulties and challenges for the widespread commercial applications of S-TENGs are analyzed and discussed from the perspectives of deepening fundamental theory, service life, electric output performance, conversion efficiency, harsh marine environment and application occasions, as shown in Fig. 12. And each of this is composed of several factors and interacts with each other.

- (1) **Deepen fundamental theory**: Although the body knowledge on the mechanism on S-TENGs, including structural design of S-TENGs [144], the general case where moving dielectric rolls in the interior of S-TENGs [145], energy optimization of a mirror-symmetric S-TENGs [146] and quantitative calculation of output power [147], has been explored, unknown knowledge of S-TENGs concerning the various inner structure of S-TENG devices that may be commercialized such as dense point contact structure and charge-shuttling needs to be exploited. To fully understand the potential of S-TENGs, it is essential for exploring a deepening fundamental theory of inherent material properties, inner structural characteristics, and connection of S-TENG-based network for S-TENGs' principles. For instances, how to provide the guidance for improving the average power of S-TENGs with unique dense point contact structure and obtaining the stable output in the long operation time after one triggering. However, the mature and comprehensive deepening fundamental knowledge concerning the above three aspects are not established. In future, fundamental theory on S-TENGs must be deepened.
- (2) **Service life**: Threaten the service life of S-TENGs relies on many internal and external impacting factors. Clearly, a key consideration of long service life along with high electric output devices mainly involves the development of wearable resistance materials (including PTFE and FEP), non-contact structural designing and practical encapsulation technology. Especially the middle, it can avoid the reciprocating frictions of the tribo-material owing to the non-contact structure. The excellent encapsulation technology is helpful to prevent the corrosion of seawater and growth of microorganism for S-TENGs. However, the present encapsulation materials, such as ethoxyline resin, cannot satisfy the commercial application. From now on, researchers should pay more attention to novel non-contact structure that can avoid the damage of tribo-materials and design the novel non-contact structure along with the practical encapsulation technology while maintaining the excellent electric output. It is noted that the service life of S-TENGs in harsh ocean environment is still a key issue in future.
- (3) **Electric output performance**: Stable and good electric outputs are the premise of achieving the commercial application. And stable and good output can be obtained by charge injection and self-charge excitation as well as and the long operation time after one triggering. These result from special inner structure, that are often introduced into S-TENGs to enhance the working stability. For instance, a high performance S-TENG having C-S main TENG based on charge-shuttling effect in S-TENGs without continuous charge injection achieves the ultra-high charge transfer amount of 7530 nC under the ultra-long operation time of 190 s [119], confirming that a stable and high output of shuttled charges is attainable. Moreover, interface circuit is also an important part in obtaining high and stable electric output. Also, it has been realized the high frequency output, enhancing the electric output and storing the energy by novel circuit design, as illustrated in Section 3.4. Nowadays, toward how to integrate these novel interface circuits and S-TENGs is the future trend. High charge density can obtain the good electric output, in which can be achieved by the method of unique polymer materials with better electronegativity

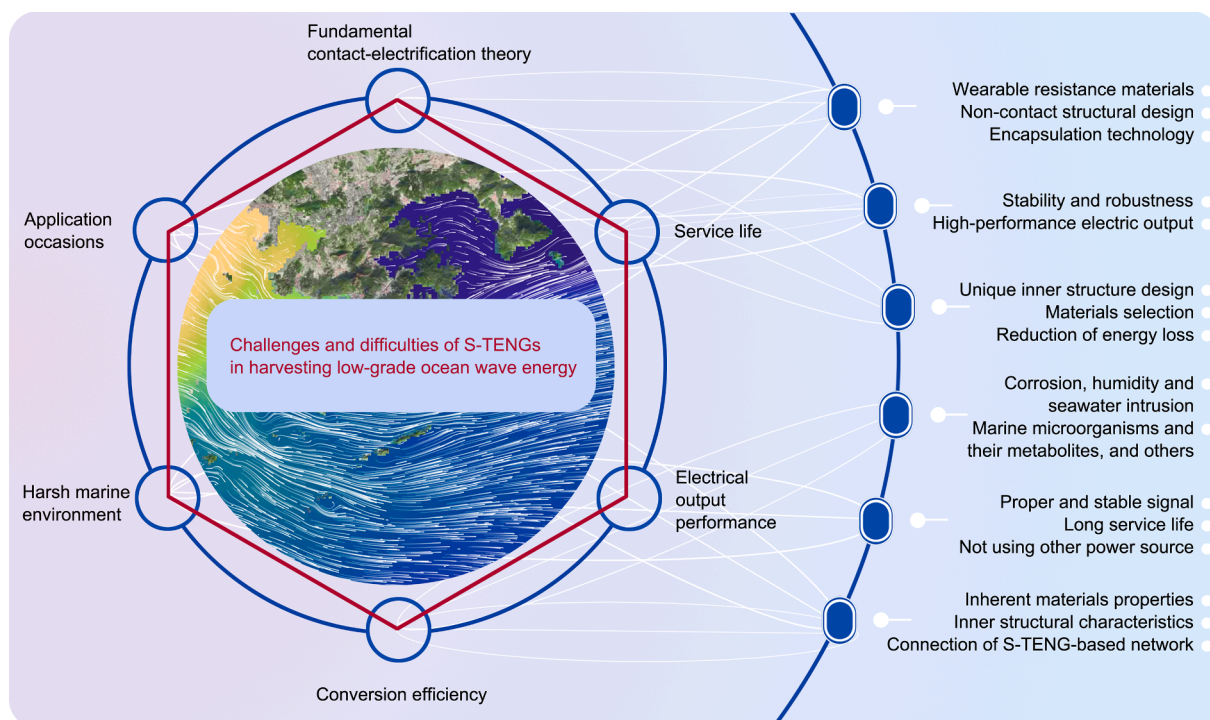


Fig. 12. Potential challenges and difficulties of S-TENGs. There show eight aspects for potential difficulties and challenges of S-TENGs and totally eighteen detailed questions on eight aspects.

or other factors except for charge injection and self-charge excitation. There are still the challenges to achieving large-scale applications in the future.

- (4) **Conversion efficiency:** Conversion efficiency is an important index to show the good or bad for the performance of triboelectric nanogenerators. Thus, the augment of conversion efficiency is crucial for realizing the large-size application. High conversion efficiency results from inner structural design, materials selection and reduction of energy loss. In the previous work, introduction of spring and proper mass of floating body in multilayer structure acts as a main role in enhancing conversion efficiency, resulting in the storage of the elastic potential energy and elevated sensitivity to full contact with the water surface. To date, there shows the highest available conversion efficiency of 14.5 % with the introduction of springs [112]. It is the typical example of designing a novel structure. Subsequently, we should comply with the principle of storing the elastic potential energy to develop the novel inner structure and showing the excellent sensitiveness to the HE-OWE. The polymer materials having eminent electronegativity can obtain the high electric output in the same external environment, indicating the outstanding capability from external low frequency mechanical energy triggering to electric energy. Developing the optimization of power management circuit plays a direct role in enhancing energy conversion efficiency by reducing energy loss. This is the key chain for HE-OWE energy conversion and facilitating the effective integration of the TENG with other energy harvesting technologies.
- (5) **Harsh marine environment:** Harsh marine environment contains huge temperature difference, corrosion, humidity, seawater intrusion, marine microorganisms, attached organisms and metabolites as well as seaquake. So better encapsulated technology, corrosion resistant materials are required to be adopted. In addition, inhibiting the growth of microorganism, including disrupting the growth conditions and preventing the growth of microorganisms, serves as a crucial part in withstanding harsh

marine environment. However, the relative research is so less. In future, we should pay more attention to create the nutrient-poor environment is essential by controlling the emission of phosphorus and nitrogen, changing the cycles of nitrogen [148]. This requires us to deeply explore the harsh environment of the ocean.

- (6) **Application occasions:** S-TENGs are mainly used in the fields of harvesting the HE-OWE and self-powered sensing. The premise of commercial application possesses stable and proper electric output, long service life and high energy conversion efficiency. Meanwhile, the high performance S-TENG by charge shuttling has the eminent electric output, realizing the that is very close to the commercial application. It cannot depend on the other power source. And S-TENG can harvest HE-OWE efficiently in a multi-dimensional motion environment. Meanwhile, it has the specific advantages, such as simple structure, encapsulation more easily, the diversity of inner structure and maintaining more easily, etc. However, much of issues such as proper and stable electric signal processing and transmission as well as long service life are not yet well addressed. So that, much effort should be devoted to achieve the above difficulties for the widespread application of S-TENGs in the near future.

In addition, SWOT (Strength, Weakness, Opportunity and Threats) analysis are adopted, as shown in Table 4. During the developing process of S-TENGs, strength, weakness, opportunity and threats is coexisted, which is elaborated in detail in Table 4. In a word, despite the difficulties and challenges remain, it is firmly believed that the existent challenges of developing HE-OWE will be well overcome in the near future, perhaps relieving the energy crisis and achieving the goal of carbon neutrality.

CRediT authorship contribution statement

Junjie Cui: Writing – review & editing, Investigation, Data curation.
Hao Li: Visualization, Methodology, Formal analysis.
Baodong Chen: Writing – review & editing, Funding acquisition.
Zhong Lin Wang: Writing – review & editing, Supervision, Conceptualization.

Table 4
Strength, Weakness, Opportunities and Threats of S-TENGs that must be faced.

| | Strength | Weakness |
|--------------------|--|--|
| Opportunity | Opportunity- Strength 1. Relieving the energy crisis 2. Relieving the dependence on fossil fuels by developing the ocean wave energy largely 3. Achieving the goal of carbon neutrality | Opportunity-Weakness 1. Not providing the guidance of structural design due to imperfect theory 2. Unstable and poor electric output as well as short service life |
| Threats | Threats- Strength 1. In fancy even if existence of strength 2. Conquering the harsh marine environment | Threats-Weakness 1. Harsh marine environment 2. Practical encapsulation technology 3. Integrating with the other fields |

Declaration of competing interest

The authors declare that they have no known competing financial interests or personal relationships that could have appeared to influence the work reported in this paper.

Data availability

Data will be made available on request.

Acknowledgments

J. C., and H. L., contributed equally to this work. This work is supported by The National Key Research and Development Program of China (Grant No. 2023YFB2604600).

References

- [1] D. Gielen, F. Boshell, D. Saygin, Climate and energy challenges for materials science, *Nat. Mater.* 15 (2016) 117–120, <https://doi.org/10.1038/nmat4545>.
- [2] Z.L. Wang, J. Chen, L. Long, Progress in triboelectric nanogenerators as a new energy technology and self-powered sensors, *Energy Environ. Sci.* 8 (2015) 2250–2282.
- [3] C.G. Granqvist, *Solar energy materials*, *Appl. Phys. A* (1991).
- [4] B. Shi, Q. Wang, H. Su, J. Li, B. Xie, P. Wang, J. Qiu, C. Wu, Y. Zhang, X. Zhou, T. W. Kim, Progress in recent research on the design and use of triboelectric nanogenerators for harvesting wind energy, *Nano Energy* 116 (2023) 108789, <https://doi.org/10.1016/j.nanoen.2023.108789>.
- [5] J. Liu, B. Bao, J. Chen, Y. Wu, Q. Wang, Marine energy harvesting from tidal currents and offshore winds: a 2-DOF system based on flow-induced vibrations, *Nano Energy* 114 (2023) 108664, <https://doi.org/10.1016/j.nanoen.2023.108664>.
- [6] Z. Fang, J. Wang, H. Wu, Q. Li, S. Fan, J. Wang, Progress and challenges of flexible lithium ion batteries, *J. Power Sources.* 454 (2020) 227932, <https://doi.org/10.1016/j.jpowsour.2020.227932>.
- [7] Y. An, Y. Tian, J. Feng, Y. Qian, MXenes for advanced separator in rechargeable batteries, *Mater. Today.* 57 (2022) 146–179, <https://doi.org/10.1016/j.mattod.2022.06.006>.
- [8] K. Fic, A. Platek, J. Piwek, E. Frackowiak, Sustainable materials for electrochemical capacitors, *Mater. Today.* 21 (2018) 437–454, <https://doi.org/10.1016/j.mattod.2018.03.005>.
- [9] A. Chen, C. Zhang, G. Zhu, Z.L. Wang, Polymer Materials for High-Performance Triboelectric Nanogenerators, *Adv. Sci.* 7 (2020) 2000186, <https://doi.org/10.1002/advs.202000186>.
- [10] K. Zhang, Y. Wang, Y. Yang, Structure Design and Performance of Hybridized Nanogenerators, *Adv. Funct. Mater.* 29 (2019) 1806435, <https://doi.org/10.1002/adfm.201806435>.
- [11] Z.L. Wang, T. Jiang, L. Xu, Toward the blue energy dream by triboelectric nanogenerator networks, *Nano Energy* 39 (2017) 9–23, <https://doi.org/10.1016/j.nanoen.2017.06.035>.
- [12] H. Zhai, S. Ding, X. Chen, Y. Wu, Z. Lin Wang, Advances in solid–solid contacting triboelectric nanogenerator for ocean energy harvesting, *Mater. Today.* 65 (2023) 166–188, <https://doi.org/10.1016/j.mattod.2023.02.030>.
- [13] O. Ellabban, H. Abu-Rub, F. Blaabjerg, Renewable energy resources: current status, future prospects and their enabling technology, *Renew. Sustain. Energy Rev.* 39 (2014) 748–764, <https://doi.org/10.1016/j.rser.2014.07.113>.
- [14] T. Dip, R. Arin, H. Anik, M.M. Uddin, S. Tushar, A. Sayam, S. Sharma, Triboelectric nanogenerators for marine applications: recent advances in energy harvesting, monitoring, and self-powered equipment, *Adv. Mater. Technol.* 8 (2023), <https://doi.org/10.1002/admt.202300802>.
- [15] S. Radhakrishnan, S. Joseph, E.J. Jelmy, K.J. Saji, T. Sanathanakrishnan, H. John, Triboelectric nanogenerators for marine energy harvesting and sensing applications, *Results Eng.* 15 (2022) 100487, <https://doi.org/10.1016/j.rineng.2022.100487>.
- [16] F. Shen, Z. Li, H. Guo, Z. Yang, H. Wu, M. Wang, J. Luo, S. Xie, Y. Peng, H. Pu, Recent advances towards ocean energy harvesting and self-powered applications based on triboelectric nanogenerators, *Adv. Electron. Mater.* 7 (2021) 2100277, <https://doi.org/10.1002/aem.202100277>.
- [17] B. Zhang, L. He, J. Wang, Y. Liu, X. Xue, S. He, C. Zhang, Z. Zhao, L. Zhou, J. Wang, Z.L. Wang, Self-powered recycling of spent lithium iron phosphate batteries via triboelectric nanogenerator, *Energy Environ. Sci.* 16 (2023) 3873–3884, <https://doi.org/10.1039/D3EE01156A>.
- [18] B. Cao, P. Wang, P. Rui, X. Wei, Z. Wang, Y. Yang, X. Tu, C. Chen, Z. Wang, Z. Yang, T. Jiang, J. Cheng, Z.L. Wang, Broadband and output-controllable triboelectric nanogenerator enabled by coupling swing-rotation switching mechanism with potential energy storage/release strategy for low-frequency mechanical energy harvesting, *Adv. Energy Mater.* 12 (2022) 2202627, <https://doi.org/10.1002/aenm.202202627>.
- [19] R. Walden, C. Kumar, D.M. Mulvihill, S.C. Pillai, Opportunities and challenges in triboelectric nanogenerator (TENG) based sustainable energy generation technologies: a mini-review, *Chem. Eng. J. Adv.* 9 (2022) 100237, <https://doi.org/10.1016/j.cej.2021.100237>.
- [20] B. Jiang, Y. Long, X. Pu, W. Hu, Z.L. Wang, A stretchable, harsh condition-resistant and ambient-stable hydrogel and its applications in triboelectric nanogenerator, *Nano Energy* 86 (2021) 106086, <https://doi.org/10.1016/j.nanoen.2021.106086>.
- [21] T. Zhao, M. Xu, X. Xiao, Y. Ma, Z. Li, Z.L. Wang, Recent progress in blue energy harvesting for powering distributed sensors in ocean, *Nano Energy* 88 (2021) 106199, <https://doi.org/10.1016/j.nanoen.2021.106199>.
- [22] Y. Yang, L. Zheng, J. Wen, F. Xing, H. Liu, Y. Shang, Z.L. Wang, B. Chen, A Swing self-regulated triboelectric nanogenerator for high-entropy ocean breaking waves energy harvesting, *Adv. Funct. Mater.* 33 (2023) 2304366, <https://doi.org/10.1002/adfm.202304366>.
- [23] S. Tian, X. Wei, L. Lai, B. Li, Z. Wu, Y. Dai, Frequency modulated hybrid nanogenerator for efficient water wave energy harvesting, *Nano Energy* 102 (2022) 107669, <https://doi.org/10.1016/j.nanoen.2022.107669>.
- [24] J. Wang, L. Pan, H. Guo, B. Zhang, R. Zhang, Z. Wu, C. Wu, L. Yang, R. Liao, Z. L. Wang, Rational structure optimized hybrid nanogenerator for highly efficient water wave energy harvesting, *Adv. Energy Mater.* 9 (2019) 1802892, <https://doi.org/10.1002/aenm.201802892>.
- [25] Z.L. Wang, On Maxwell's displacement current for energy and sensors: the origin of nanogenerators, *Mater. Today.* 20 (2017) 74–82, <https://doi.org/10.1016/j.mattod.2016.12.001>.
- [26] Y. Su, X. Wen, G. Zhu, J. Yang, J. Chen, P. Bai, Z. Wu, Y. Jiang, Z. Lin Wang, Hybrid triboelectric nanogenerator for harvesting water wave energy and as a self-powered distress signal emitter, *Nano Energy* 9 (2014) 186–195, <https://doi.org/10.1016/j.nanoen.2014.07.006>.
- [27] A. Jouanne, Harvesting the Waves, *Mech. Eng.* 128 (2006) 24–27, <https://doi.org/10.1115/1.2006-DEC-1>.
- [28] S. Panda, S. Hajra, Y. Oh, W. Oh, J. Lee, H. Shin, V. Vivekananthan, Y. Yang, Y. K. Mishra, H.J. Kim, Hybrid nanogenerators for ocean energy harvesting: mechanisms designs, and applications, *Small.* 19 (2023) 2300847, <https://doi.org/10.1002/smll.202300847>.
- [29] Y. Feng, X. Liang, J. An, T. Jiang, Z.L. Wang, Soft-contact cylindrical triboelectric-electromagnetic hybrid nanogenerator based on swing structure for ultra-low frequency water wave energy harvesting, *Nano Energy* 81 (2021) 105625, <https://doi.org/10.1016/j.nanoen.2020.105625>.
- [30] B. Zhang, W. Li, J. Ge, C. Chen, X. Yu, Z.L. Wang, T. Cheng, Single-material-substrated triboelectric–electromagnetic hybrid generator for self-powered multifunctional sensing in intelligent greenhouse, *Nano Res.* 16 (2023) 3149–3155, <https://doi.org/10.1007/s12274-022-4922-1>.
- [31] M. Xu, S. Wang, S.L. Zhang, W. Ding, P.T. Kien, C. Wang, Z. Li, X. Pan, Z.L. Wang, A highly-sensitive wave sensor based on liquid-solid interfacing triboelectric nanogenerator for smart marine equipment, *Nano Energy* 57 (2019) 574–580, <https://doi.org/10.1016/j.nanoen.2018.12.041>.
- [32] W. Zhong, L. Xu, X. Yang, W. Tang, J. Shao, B. Chen, Z.L. Wang, Open-book-like triboelectric nanogenerators based on low-frequency roll–swing oscillators for wave energy harvesting, *Nanoscale* 11 (2019) 7199–7208, <https://doi.org/10.1039/C8NR09978B>.
- [33] T. Cheng, J. Shao, Z.L. Wang, Triboelectric nanogenerators, *Nature Rev. Methods Primers.* 3 (2023) 39, <https://doi.org/10.1038/s43586-023-00220-3>.
- [34] B. Chen, Z.L. Wang, Toward a new era of sustainable energy: advanced triboelectric nanogenerator for harvesting high entropy energy, *Small* 18 (2022) 2107034, <https://doi.org/10.1002/smll.202107034>.
- [35] B. Chen, W. Tang, Z.L. Wang, Advanced 3D printing-based triboelectric nanogenerator for mechanical energy harvesting and self-powered sensing, *Mater. Today.* 50 (2021) 224–238, <https://doi.org/10.1016/j.mattod.2021.05.017>.
- [36] J. Luo, Z.L. Wang, Recent progress of triboelectric nanogenerators: from fundamental theory to practical applications, *EcoMat.* 2 (2020) e12059.
- [37] J. Shao, M. Willatzen, T. Jiang, W. Tang, X. Chen, J. Wang, Z.L. Wang, Quantifying the power output and structural figure-of-merits of triboelectric nanogenerators in a charging system starting from the Maxwell's displacement current, *Nano Energy* 59 (2019) 380–389, <https://doi.org/10.1016/j.nanoen.2019.02.051>.

- [38] S. Niu, Z.L. Wang, Theoretical systems of triboelectric nanogenerators, *Nano Energy* 14 (2015) 161–192, <https://doi.org/10.1016/j.nanoen.2014.11.034>.
- [39] F. Fan, Z. Tian, Z. Lin Wang, Flexible triboelectric generator, *Nano Energy* 1 2012 328–334. [10.1016/j.nanoen.2012.01.004](https://doi.org/10.1016/j.nanoen.2012.01.004).
- [40] Z.L. Wang, Catch wave power in floating nets, *Nature* 542 (2017) 159–160, <https://doi.org/10.1038/542159a>.
- [41] Y. Jiang, X. Liang, T. Jiang, Z.L. Wang, Advances in triboelectric nanogenerators for blue energy harvesting and marine environmental monitoring, *Engineering* 33 (2024) 204–224, <https://doi.org/10.1016/j.eng.2023.05.023>.
- [42] Z. Saadatnia, E. Asadi, H. Askari, J. Zu, E. Esmailzadeh, Modeling and performance analysis of duck-shaped triboelectric and electromagnetic generators for water wave energy harvesting, *Int. J. Energy Res.* 41 (2017) 2392–2404, <https://doi.org/10.1002/er.3811>.
- [43] J. Chen, J. Yang, Z. Li, X. Fan, Y. Qi, Q. Jing, H. Guo, Z. Wen, K.C. Pradel, S. Niu, Z.L. Wang, Networks of triboelectric nanogenerators for harvesting water wave energy: a potential approach toward blue energy, *ACS Nano* 9 (2015) 3324–3331, <https://doi.org/10.1021/acsnano.5b00534>.
- [44] Q. Xu, C. Shang, H. Ma, Q. Hong, C. Li, S. Ding, L. Xue, X. Sun, Y. Pan, T. Sugahara, Y. Yalikun, Y. Lai, Y. Yang, A guided-liquid-based hybrid triboelectric nanogenerator for omnidirectional and high-performance ocean wave energy harvesting, *Nano Energy* 109 (2023) 108240, <https://doi.org/10.1016/j.nanoen.2023.108240>.
- [45] D. Zhao, H. Li, Y. Yu, Y. Wang, J. Wang, Q. Gao, Z.L. Wang, J. Wen, T. Cheng, A current-enhanced triboelectric nanogenerator with crossed rollers for harvesting wave energy, *Nano Energy* 117 (2023) 108885, <https://doi.org/10.1016/j.nanoen.2023.108885>.
- [46] Y. Hu, H. Qiu, Q. Sun, Z.L. Wang, L. Xu, Wheel-structured triboelectric nanogenerators with hyperelastic networking for high-performance wave energy harvesting, *Small Methods* 7 (2023) 2300582, <https://doi.org/10.1002/smt.202300582>.
- [47] S.L. Zhang, M. Xu, C. Zhang, Y. Wang, H. Zou, X. He, Z. Wang, Z.L. Wang, Rationally designed sea snake structure based triboelectric nanogenerators for effectively and efficiently harvesting ocean wave energy with minimized water screening effect, *Nano Energy* 48 (2018) 421–429, <https://doi.org/10.1016/j.nanoen.2018.03.062>.
- [48] Y. Zou, M. Sun, S. Li, X. Zhang, L. Feng, Y. Wang, T. Du, Y. Ji, P. Sun, M. Xu, Advances in self-powered triboelectric sensor toward marine IoT, *Nano Energy* 122 (2024) 109316, <https://doi.org/10.1016/j.nanoen.2024.109316>.
- [49] J. Han, Y. Liu, Y. Feng, T. Jiang, Z.L. Wang, Achieving a large driving force on triboelectric nanogenerator by wave-driven linkage mechanism for harvesting blue energy toward marine environment monitoring, *Adv. Energy Mater.* 13 (2023) 2203219, <https://doi.org/10.1002/aenm.202203219>.
- [50] D. Liu, C. Li, P. Chen, X. Zhao, W. Tang, Z.L. Wang, Sustainable long-term and wide-area environment monitoring network based on distributed self-powered wireless sensing nodes, *Adv. Energy Mater.* 13 (2023) 2202691, <https://doi.org/10.1002/aenm.202202691>.
- [51] Y.F. Wang, B. Cao, Y.W. Yang, Y. Yu, P.H. Wang, C.C. Wang, Multi-channel self-powered attitude sensor based on triboelectric nanogenerator and inertia, *Nano Energy* 107 (2023) 108164, <https://doi.org/10.1016/j.nanoen.2022.108164>.
- [52] X. Wang, J. Liu, S. Wang, J. Zheng, T. Guan, X. Liu, T. Wang, T. Chen, H. Wang, G. Xie, P. Xu, J. Tao, M. Xu, A self-powered triboelectric coral-like sensor integrated buoy for irregular and ultra-low frequency ocean wave monitoring, *Adv. Mater. Technol.* 7 (2022) 2101098, <https://doi.org/10.1002/admt.202101098>.
- [53] Q. Zhang, C. Xin, F. Shen, Y. Gong, Y. Zi, H. Guo, Z. Li, Y. Peng, Q. Zhang, Z. L. Wang, Human body IoT systems based on the triboelectrification effect: energy harvesting, sensing, interfacing and communication, *Energy Environ. Sci.* 15 (2022) 3688–3721, <https://doi.org/10.1039/D2EE01590K>.
- [54] Z. Ren, X. Liang, D. Liu, X. Li, J. Ping, Z. Wang, Z.L. Wang, Water-wave driven route avoidance warning system for wireless ocean navigation, *Adv. Energy Mater.* 11 (2021) 2101116, <https://doi.org/10.1002/aenm.202101116>.
- [55] H. Pang, Y. Feng, J. An, P. Chen, J. Han, T. Jiang, Z.L. Wang, Segmented swing-structured fur-based triboelectric nanogenerator for harvesting blue energy toward marine environmental applications, *Adv. Funct. Mater.* 31 (2021) 2106398, <https://doi.org/10.1002/adfm.202106398>.
- [56] A. Ahmed, I. Hassan, M.F. El-Kady, A. Radhi, C.K. Jeong, P.R. Selvaganapathy, J. Zu, S. Ren, Q. Wang, R.B. Kaner, Integrated triboelectric nanogenerators in the era of the internet of things, *Adv. Sci.* 6 (2019) 1802230, <https://doi.org/10.1002/advs.201802230>.
- [57] M. Yeh, H. Guo, L. Lin, Z. Wen, Z. Li, C. Hu, Z.L. Wang, Rolling friction enhanced free-standing triboelectric nanogenerators and their applications in self-powered electrochemical recovery systems, *Adv. Funct. Mater.* 26 (2016) 1054–1062, <https://doi.org/10.1002/adfm.201504396>.
- [58] X. Wang, Q. Gao, M. Zhu, J. Wang, J. Zhu, H. Zhao, Z.L. Wang, T. Cheng, Bioinspired butterfly wings triboelectric nanogenerator with drag amplification for multidirectional underwater-wave energy harvesting, *Appl. Energy* 323 (2022) 119648, <https://doi.org/10.1016/j.apenergy.2022.119648>.
- [59] C. Zhang, W. Yuan, B. Zhang, J. Yang, Y. Hu, L. He, X. Zhao, X. Li, Z.L. Wang, J. Wang, A rotating triboelectric nanogenerator driven by bidirectional swing for water wave energy harvesting, *Small* 19 (2023) 2304412, <https://doi.org/10.1002/sml.202304412>.
- [60] X. Sun, C. Shang, H. Ma, C. Li, L. Xue, Q. Xu, Z. Wei, W. Li, Y. Yalikun, Y. Lai, Y. Yang, A tube-shaped solid-liquid-interfaced triboelectric-electromagnetic hybrid nanogenerator for efficient ocean wave energy harvesting, *Nano Energy* 100 (2022) 107540, <https://doi.org/10.1016/j.nanoen.2022.107540>.
- [61] T. Jiang, H. Pang, J. An, P. Lu, Y. Feng, X. Liang, W. Zhong, Z.L. Wang, Robust swing-structured triboelectric nanogenerator for efficient blue energy harvesting, *Adv. Energy Mater.* 10 (2020) 2000064, <https://doi.org/10.1002/aenm.202000064>.
- [62] Y. Feng, T. Jiang, X. Liang, J. An, Z.L. Wang, Cylindrical triboelectric nanogenerator based on swing structure for efficient harvesting of ultra-low-frequency water wave energy, *Appl. Phys. Rev.* 7 (2020) 21401, <https://doi.org/10.1063/1.5135734>.
- [63] W. Li, L. Wan, Y. Lin, G. Liu, H. Qu, H. Wen, J. Ding, H. Ning, H. Yao, Synchronous nanogenerator with intermittent sliding friction self-excitation for water wave energy harvesting, *Nano Energy* 95 (2022) 106994, <https://doi.org/10.1016/j.nanoen.2022.106994>.
- [64] P. Rui, W. Zhang, Y. Zhong, X. Wei, Y. Guo, S. Shi, Y. Liao, J. Cheng, P. Wang, High-performance cylindrical pendulum shaped triboelectric nanogenerators driven by water wave energy for full-automatic and self-powered wireless hydrological monitoring system, *Nano Energy* 74 (2020) 104937, <https://doi.org/10.1016/j.nanoen.2020.104937>.
- [65] C. Rodrigues, M. Ramos, R. Esteves, J. Correia, D. Clemente, F. Gonçalves, N. Mathias, M. Gomes, J. Silva, C. Duarte, T. Morais, P. Rosa-Santos, F. Taveira-Pinto, A. Pereira, J. Ventura, Integrated study of triboelectric nanogenerator for ocean wave energy harvesting: performance assessment in realistic sea conditions, *Nano Energy* 84 (2021) 105890, <https://doi.org/10.1016/j.nanoen.2021.105890>.
- [66] J. Tan, S. Sun, D. Jiang, M. Xu, X. Chen, Y. Song, Z.L. Wang, Advances in triboelectric nanogenerator powered electrowetting-on-dielectric devices: mechanism, structures, and applications, *Mater. Today* 58 (2022) 201–220, <https://doi.org/10.1016/j.mattod.2022.07.009>.
- [67] X. Wei, Z. Zhao, C. Zhang, W. Yuan, Z. Wu, J. Wang, Z.L. Wang, All-Weather droplet-based triboelectric nanogenerator for wave energy harvesting, *ACS Nano* 15 (2021) 13200–13208, <https://doi.org/10.1021/acsnano.1c02790>.
- [68] Y. Yang, X. Yu, L. Meng, X. Li, Y. Xu, T. Cheng, S. Liu, Z.L. Wang, Triboelectric nanogenerator with double rocker structure design for ultra-low-frequency wave full-stroke energy harvesting, *Extreme Mech. Lett.* 46 (2021) 101338, <https://doi.org/10.1016/j.eml.2021.101338>.
- [69] F. Huang, P. Yang, Z. Liu, D. Yang, L. Huang, Y. Shi, X. Tao, Y. Chen, H. Li, X. Chen, Z. Bian, A hybrid nanogenerator for collecting both water wave and steam evaporation energy, *Nano Energy* 110 (2023) 108346, <https://doi.org/10.1016/j.nanoen.2023.108346>.
- [70] R. Lei, H. Zhai, J. Nie, W. Zhong, Y. Bai, X. Liang, L. Xu, T. Jiang, X. Chen, Z. L. Wang, Butterfly-inspired triboelectric nanogenerators with spring-assisted linkage structure for water wave energy harvesting, *Adv. Mater. Technol.* 4 (2019) 1800514, <https://doi.org/10.1002/admt.201800514>.
- [71] T. Jiang, Y. Yao, L. Xu, L. Zhang, T. Xiao, Z.L. Wang, Spring-assisted triboelectric nanogenerator for efficiently harvesting water wave energy, *Nano Energy* 31 (2017) 560–567, <https://doi.org/10.1016/j.nanoen.2016.12.004>.
- [72] W. Liu, L. Xu, T. Bu, H. Yang, G. Liu, W. Li, Y. Pang, C. Hu, C. Zhang, T. Cheng, Torus structured triboelectric nanogenerator array for water wave energy harvesting, *Nano Energy* 58 (2019) 499–507, <https://doi.org/10.1016/j.nanoen.2019.01.088>.
- [73] C. Zhang, W. Yuan, B. Zhang, O. Yang, Y. Liu, L. He, J. Wang, Z.L. Wang, High space efficiency hybrid nanogenerators for effective water wave energy harvesting, *Adv. Funct. Mater.* 32 (2022) 2111775, <https://doi.org/10.1002/adfm.202111775>.
- [74] L.M. Zhang, C.B. Han, T. Jiang, T. Zhou, X.H. Li, C. Zhang, Z.L. Wang, Multilayer wavy-structured robust triboelectric nanogenerator for harvesting water wave energy, *Nano Energy* 22 (2016) 87–94, <https://doi.org/10.1016/j.nanoen.2016.01.009>.
- [75] B. Zhu, H. Wu, H. Wang, Z. Quan, H. Luo, L. Yang, R. Liao, J. Wang, Spherical 3D fractal structured dual-mode triboelectric nanogenerator for multidirectional low-frequency wave energy harvesting, *Nano Energy* 124 (2024) 109446, <https://doi.org/10.1016/j.nanoen.2024.109446>.
- [76] X. Li, X. Yin, Z. Zhao, L. Zhou, D. Liu, C. Zhang, C. Zhang, W. Zhang, S. Li, J. Wang, Z.L. Wang, Long-lifetime triboelectric nanogenerator operated in conjunction modes and low crest factor, *Adv. Energy Mater.* 10 (2020) 1903024, <https://doi.org/10.1002/aenm.201903024>.
- [77] Y. Bai, L. Xu, C. He, L. Zhu, X. Yang, T. Jiang, J. Nie, W. Zhong, Z.L. Wang, High-performance triboelectric nanogenerators for self-powered, in-situ and real-time water quality mapping, *Nano Energy* 66 (2019) 104117, <https://doi.org/10.1016/j.nanoen.2019.104117>.
- [78] X. Li, J. Tao, X. Wang, J. Zhu, C. Pan, Z.L. Wang, Networks of high performance triboelectric nanogenerators based on liquid-solid interface contact electrification for harvesting low-frequency blue energy, *Adv. Energy Mater.* 8 (2018) 1800705, <https://doi.org/10.1002/aenm.201800705>.
- [79] T. Jiang, L.M. Zhang, X. Chen, C.B. Han, W. Tang, C. Zhang, L. Xu, Z.L. Wang, Structural optimization of triboelectric nanogenerator for harvesting water wave energy, *ACS Nano* 9 (2015) 12562–12572, <https://doi.org/10.1021/acsnano.5b06372>.
- [80] Y. Xu, W. Yang, X. Lu, Y. Yang, J. Li, J. Wen, T. Cheng, Z.L. Wang, Triboelectric nanogenerator for ocean wave graded energy harvesting and condition monitoring, *ACS Nano* 15 (2021) 16368–16375, <https://doi.org/10.1021/acsnano.1c05685>.
- [81] J. Ren, C. Gao, J. An, Q. Liu, J. Wang, T. Jiang, Z.L. Wang, Arc-shaped triboelectric nanogenerator based on rolling structure for harvesting low-frequency water wave energy, *Adv. Mater. Technol.* 6 (2021) 2100359, <https://doi.org/10.1002/admt.202100359>.

- [82] A. Wang, J. Chen, L. Wang, J. Han, W. Su, A. Li, P. Liu, L. Duan, C. Xu, Z. Zeng, Numerical analysis and experimental study of an ocean wave tetrahedral triboelectric nanogenerator, *Appl. Energy*. 307 (2022) 118174, <https://doi.org/10.1016/j.apenergy.2021.118174>.
- [83] Y. Xi, J. Wang, Y. Zi, X. Li, C. Han, X. Cao, C. Hu, Z. Wang, High efficient harvesting of underwater ultrasonic wave energy by triboelectric nanogenerator, *Nano Energy* 38 (2017) 101–108, <https://doi.org/10.1016/j.nanoen.2017.04.053>.
- [84] X. Liang, S. Liu, S. Lin, H. Yang, T. Jiang, Z.L. Wang, Liquid-solid triboelectric nanogenerator arrays based on dynamic electric-double-layer for harvesting water wave energy, *Adv. Energy Mater.* 13 (2023) 2300571, <https://doi.org/10.1002/aenm.202300571>.
- [85] L. Liu, Q. Shi, J.S. Ho, C. Lee, Study of thin film blue energy harvester based on triboelectric nanogenerator and seashore IoT applications, *Nano Energy* 66 (2019) 104167, <https://doi.org/10.1016/j.nanoen.2019.104167>.
- [86] B.D. Chen, W. Tang, C. He, C.R. Deng, L.J. Yang, L.P. Zhu, J. Chen, J.J. Shao, L. Liu, Z.L. Wang, Water wave energy harvesting and self-powered liquid-surface fluctuation sensing based on bionic-jellyfish triboelectric nanogenerator, *Mater. Today*. 21 (2018) 88–97, <https://doi.org/10.1016/j.mattod.2017.10.006>.
- [87] J. Ding, J. Jiang, T. Lin, G. Liu, H. Yao, H. Wen, S. Li, F. Mo, L. Wan, Realization of a sustainable charging power source by in situ low-frequency water wave energy harvesting with a coaxial triboelectric-electromagnetic hybrid generator, *Adv. Energy Sustain. Res.* 3 (2022) 2200087, <https://doi.org/10.1002/aesr.202200087>.
- [88] K. Xia, J. Fu, Z. Xu, Multiple-frequency high-output triboelectric nanogenerator based on a water balloon for all-weather water wave energy harvesting, *Adv. Energy Mater.* 10 (2020) 2000426, <https://doi.org/10.1002/aenm.202000426>.
- [89] G. Zhu, Y. Su, P. Bai, J. Chen, Q. Jing, W. Yang, Z.L. Wang, Harvesting water wave energy by asymmetric screening of electrostatic charges on a nanostructured hydrophobic thin-film surface, *ACS Nano* 8 (2014) 6031–6037, <https://doi.org/10.1021/nn501273z>.
- [90] H. Chen, J. Wang, A. Ning, Optimization of a rolling triboelectric nanogenerator based on the nano-micro structure for ocean environmental monitoring, *ACS Omega* 6 (2021) 21059–21065, <https://doi.org/10.1021/acsomega.1c02709>.
- [91] X. Wang, S. Niu, Y. Yin, F. Yi, Z. You, Z.L. Wang, Triboelectric nanogenerator based on fully enclosed rolling spherical structure for harvesting low-frequency water wave energy, *Adv. Energy Mater.* 5 (2015) 1501467, <https://doi.org/10.1002/aenm.201501467>.
- [92] W. Liu, L. Xu, G. Liu, H. Yang, T. Bu, X. Fu, S. Xu, C. Fang, C. Zhang, Network topology optimization of triboelectric nanogenerators for effectively harvesting ocean wave energy, *Iscience*. 23 (2020) 101848, <https://doi.org/10.1016/j.isci.2020.101848>.
- [93] P. Cheng, H. Guo, Z. Wen, C. Zhang, X. Yin, X. Li, D. Liu, W. Song, X. Sun, J. Wang, Z.L. Wang, Largely enhanced triboelectric nanogenerator for efficient harvesting of water wave energy by soft contacted structure, *Nano Energy* 57 (2019) 432–439, <https://doi.org/10.1016/j.nanoen.2018.12.054>.
- [94] L. Xu, T. Jiang, P. Lin, J.J. Shao, C. He, W. Zhong, X.Y. Chen, Z.L. Wang, Coupled triboelectric nanogenerator networks for efficient water wave energy harvesting, *ACS Nano* 12 (2018) 1849–1858, <https://doi.org/10.1021/acsnano.7b08674>.
- [95] Y. Pang, Y. Fang, J. Su, H. Wang, Y. Tan, C.C. Cao, Soft ball-based triboelectric-electromagnetic hybrid nanogenerators for wave energy harvesting, *Adv. Mater. Technol.* 8 (2023) 2201246, <https://doi.org/10.1002/admt.202201246>.
- [96] X. Li, L. Xu, P. Lin, X. Yang, H. Wang, H. Qin, Z.L. Wang, Three-dimensional chiral networks of triboelectric nanogenerators inspired by metamaterial's structure, *Energy Environ. Sci.* 16 (2023) 3040–3052, <https://doi.org/10.1039/D3EE01035J>.
- [97] W. Zhang, W. He, S. Dai, F. Ma, P. Lin, J. Sun, L. Dong, C. Hu, Wave energy harvesting based on multilayer beads integrated spherical TENG with switch triggered instant discharging for self-powered hydrogen generation, *Nano Energy* 111 (2023) 108432, <https://doi.org/10.1016/j.nanoen.2023.108432>.
- [98] Z. Yuan, C. Wang, J. Xi, X. Han, J. Li, S. Han, W. Gao, C. Pan, Spherical triboelectric nanogenerator with dense point contacts for harvesting multidirectional water wave and vibration energy, *ACS Energy Lett.* 6 (2021) 2809–2816, <https://doi.org/10.1021/acsenenergylett.1c01092>.
- [99] J. He, X. Fan, J. Mu, C. Wang, J. Qian, X. Li, X. Hou, W. Geng, X. Wang, X. Chou, 3D full-space triboelectric-electromagnetic hybrid nanogenerator for high-efficient mechanical energy harvesting in vibration system, *Energy* 194 (2020) 116871, <https://doi.org/10.1016/j.energy.2019.116871>.
- [100] X. Yang, L. Xu, P. Lin, W. Zhong, Y. Bai, J. Luo, J. Chen, Z.L. Wang, Macroscopic self-assembly network of encapsulated high-performance triboelectric nanogenerators for water wave energy harvesting, *Nano Energy* 60 (2019) 404–412, <https://doi.org/10.1016/j.nanoen.2019.03.054>.
- [101] Y. Pang, S. Chen, Y. Chu, Z.L. Wang, C. Cao, Matryoshka-inspired hierarchically structured triboelectric nanogenerators for wave energy harvesting, *Nano Energy* 66 (2019) 104131, <https://doi.org/10.1016/j.nanoen.2019.104131>.
- [102] Z. Lin, B. Zhang, H. Guo, Z. Wu, H. Zou, J. Yang, Z.L. Wang, Super-robust and frequency-multiplied triboelectric nanogenerator for efficient harvesting water and wind energy, *Nano Energy* 64 (2019) 103908, <https://doi.org/10.1016/j.nanoen.2019.103908>.
- [103] Z. Lin, B. Zhang, Y. Xie, Z. Wu, J. Yang, Z.L. Wang, Elastic-Connection and Soft-Contact Triboelectric Nanogenerator with Superior Durability and Efficiency, *Adv. Funct. Mater.* 31 (2021) 2105237, <https://doi.org/10.1002/adfm.202105237>.
- [104] J. Guo, J. He, Z. Yuan, J. Tao, X. Liu, Z. Song, W. Gao, C. Wang, C. Pan, Self-powered angle-resolved triboelectric nanogenerator for underwater vibration localization, *Nano Energy* 110 (2023) 108392, <https://doi.org/10.1016/j.nanoen.2023.108392>.
- [105] Q. Gao, Y. Xu, X. Yu, Z. Jing, T. Cheng, Z.L. Wang, Gyroscope-structured triboelectric nanogenerator for harvesting multidirectional ocean wave energy, *ACS Nano* 16 (2022) 6781–6788, <https://doi.org/10.1021/acsnano.2c01594>.
- [106] Z. Qu, M. Huang, C. Chen, Y. An, H. Liu, Q. Zhang, X. Wang, Y. Liu, W. Yin, X. Li, Spherical triboelectric nanogenerator based on eccentric structure for omnidirectional low frequency water wave energy harvesting, *Adv. Funct. Mater.* 32 (2022) 2202048, <https://doi.org/10.1002/adfm.202202048>.
- [107] Z. Wu, H. Guo, W. Ding, Y. Wang, L. Zhang, Z. Wang, A hybridized triboelectric-electromagnetic water wave energy harvester based on a magnetic sphere, *ACS Nano* 13 (2019), <https://doi.org/10.1021/acsnano.8b09088>.
- [108] Q. Shi, H. Wang, H. Wu, C. Lee, Self-powered triboelectric nanogenerator buoy ball for applications ranging from environment monitoring to water wave energy farm, *Nano Energy* 40 (2017) 203–213, <https://doi.org/10.1016/j.nanoen.2017.08.018>.
- [109] K. Tao, H. Yi, Y. Yang, H. Chang, J. Wu, L. Tang, Z. Yang, N. Wang, L. Hu, Y. Fu, J. Miao, W. Yuan, Origami-inspired electret-based triboelectric generator for biomechanical and ocean wave energy harvesting, *Nano Energy* 67 (2020) 104197, <https://doi.org/10.1016/j.nanoen.2019.104197>.
- [110] S. Liu, X. Liang, P. Chen, H. Long, T. Jiang, Z.L. Wang, Multilayered helical spherical triboelectric nanogenerator with charge shuttling for water wave energy harvesting, *Small Methods*. 7 (2023) 2201392, <https://doi.org/10.1002/smt.202201392>.
- [111] Y. Li, Z. Guo, Z. Zhao, Y. Gao, P. Yang, W. Qiao, L. Zhou, J. Wang, Z.L. Wang, Multi-layered triboelectric nanogenerator incorporated with self-charge excitation for efficient water wave energy harvesting, *Appl. Energy*. 336 (2023) 120792, <https://doi.org/10.1016/j.apenergy.2023.120792>.
- [112] X. Zhang, Q. Yang, P. Ji, Z. Wu, Q. Li, H. Yang, X. Li, G. Zheng, Y. Xi, Z.L. Wang, Modeling of liquid-solid hydrodynamic water wave energy harvesting system based on triboelectric nanogenerator, *Nano Energy* 99 (2022) 107362, <https://doi.org/10.1016/j.nanoen.2022.107362>.
- [113] X. Liang, Z. Liu, Y. Feng, J. Han, L. Li, J. An, P. Chen, T. Jiang, Z.L. Wang, Spherical triboelectric nanogenerator based on spring-assisted swing structure for effective water wave energy harvesting, *Nano Energy* 83 (2021) 105836, <https://doi.org/10.1016/j.nanoen.2021.105836>.
- [114] X. Liang, T. Jiang, G. Liu, Y. Peng, C. Zhang, Z.L. Wang, Spherical triboelectric nanogenerator integrated with power management module for harvesting multidirectional water wave energy, *Energy Environ. Sci.* 13 (2020) 277–285, <https://doi.org/10.1039/c9ee03258d>.
- [115] X. Liang, T. Jiang, G. Liu, T. Xiao, L. Xu, W. Li, F. Xi, C. Zhang, Z.L. Wang, Triboelectric nanogenerator networks integrated with power management module for water wave energy harvesting, *Adv. Funct. Mater.* 29 (2019) 1807241, <https://doi.org/10.1002/adfm.201807241>.
- [116] J. An, Z.M. Wang, T. Jiang, X. Liang, Z.L. Wang, Whirling-folded triboelectric nanogenerator with high average power for water wave energy harvesting, *Adv. Funct. Mater.* 29 (2019) 1904867, <https://doi.org/10.1002/adfm.201904867>.
- [117] T.X. Xiao, X. Liang, T. Jiang, L. Xu, J.J. Shao, J.H. Nie, Y. Bai, W. Zhong, Z. L. Wang, Spherical triboelectric nanogenerators based on spring-assisted multilayered structure for efficient water wave energy harvesting, *Adv. Funct. Mater.* 28 (2018) 1802634, <https://doi.org/10.1002/adfm.201802634>.
- [118] G. Liu, H. Guo, S. Xu, C. Hu, Z.L. Wang, Oblate spheroidal triboelectric nanogenerator for all-weather blue energy harvesting, *Adv. Energy Mater.* 9 (2019) 1900801, <https://doi.org/10.1002/aenm.201900801>.
- [119] H. Wang, L. Xu, Y. Bai, Z.L. Wang, Pumping up the charge density of a triboelectric nanogenerator by charge-shuttling, *Nat. Commun.* 11 (2020) 4203, <https://doi.org/10.1038/s41467-020-17891-1>.
- [120] H. Zou, Y. Zhang, L. Guo, P. Wang, X. He, G. Dai, H. Zheng, C. Chen, A.C. Wang, C. Xu, Z.L. Wang, Quantifying the triboelectric series, *Nat. Commun.* 10 (2019) 1427, <https://doi.org/10.1038/s41467-019-09461-x>.
- [121] S. Li, J. Nie, Y. Shi, X. Tao, F. Wang, J. Tian, S. Lin, X. Chen, Z.L. Wang, Contributions of different functional groups to contact electrification of polymers, *Adv. Mater.* 32 (2020) 2001307, <https://doi.org/10.1002/adma.202001307>.
- [122] S. Liu, Z. Hou, L. Lin, Z. Li, H. Sun, 3D laser nanoprinting of functional materials, *Adv. Funct. Mater.* 33 (2023) 2211280, <https://doi.org/10.1002/adfm.202211280>.
- [123] C. Barner-Kowollik, M. Bastmeyer, E. Blasco, G. Delaitre, P. Müller, B. Richter, M. Wegener, 3D laser micro- and nanoprinting: challenges for chemistry, *Angew. Chem. Int. Ed.* 56 (2017) 15828–15845, <https://doi.org/10.1002/anie.201704695>.
- [124] J. Carneiro De Oliveira, A. Airoudj, P. Kunemann, F. Bally-Le Gall, V. Roucoules, Mechanical properties of plasma polymer films: a review, *SN Appl. Sci.* 3 (2021) 656, <https://doi.org/10.1007/s42452-021-04655-9>.
- [125] Z.L. Wang, Triboelectric nanogenerator (TENG)—sparking an energy and sensor revolution, *Adv. Energy Mater.* 10 (2020) 2000137, <https://doi.org/10.1002/aenm.202000137>.
- [126] W. Yan, Y. Liu, P. Chen, L.N.Y. Cao, J. An, T. Jiang, W. Tang, B. Chen, Z.L. Wang, Flexible film-discharge-switch assisted universal power management system for the four operation modes of triboelectric nanogenerators, *Adv. Energy Mater.* 12 (2022) 2103677, <https://doi.org/10.1002/aenm.202103677>.
- [127] H. Liu, Y. Xu, Y. Xiao, S. Zhang, C. Qu, L. Lv, H. Chen, G. Song, Highly adaptive liquid-solid triboelectric nanogenerator-assisted self-powered water wave motion sensor, *ACS Appl. Electron. Mater.* 4 (2022) 3870–3879, <https://doi.org/10.1021/acsaelm.2c00537>.
- [128] X.J. Zhao, J.J. Tian, S.Y. Kuang, H. Ouyang, L. Yan, Z.L. Wang, Z. Li, G. Zhu, Biocide-free antifouling on insulating surface by wave-driven triboelectrification-

- induced potential oscillation, *Adv. Mater. Interfaces.* 3 (2016) 1600187, <https://doi.org/10.1002/admi.201600187>.
- [129] R.R. Tripathy, R. Sahoo, S. Mishra, B. Das, S. Balasubramaniam, A. Ramadoss, Fabrication and feasibility study of polymer-based triboelectric nanogenerator towards blue energy harvesting, *Green Energy and Resources.* 1 (2023) 100006, <https://doi.org/10.1016/j.gerr.2023.100006>.
- [130] H. Xiang, Y. Zeng, X. Huang, N. Wang, X. Cao, Z.L. Wang, From triboelectric nanogenerator to multifunctional triboelectric sensors: a chemical perspective toward the interface optimization and device integration, *Small* 18 (2022) 2107222, <https://doi.org/10.1002/smll.202107222>.
- [131] W. Yu, J. Ma, Z. Zhang, T. Ren, A novel interface circuit for triboelectric nanogenerator², *J. Semicond.* 38 (2017) 105009, <https://doi.org/10.1088/1674-4926/38/10/105009>.
- [132] S. Y., Y. M., S. Y., A Dual-Output Rectifier-Based Self-Powered Interface Circuit for Triboelectric Nanogenerators, *IEEE Trans. Power Electron.* 39 (2024) 6630-6634, <https://doi.org/10.1109/TPEL.2024.3376536>.
- [133] Y. Hu, Q. Yue, S. Lu, D. Yang, S. Shi, X. Zhang, H. Yu, An Adaptable Interface Conditioning Circuit Based on Triboelectric Nanogenerators for Self-Powered Sensors, 2018.
- [134] H. Askari, N. Xu, B.H. Groenner Barbosa, Y. Huang, L. Chen, A. Khajepour, H. Chen, Z.L. Wang, Intelligent systems using triboelectric, piezoelectric, and pyroelectric nanogenerators, *Mater. Today.* 52 (2022) 188-206, <https://doi.org/10.1016/j.mattod.2021.11.027>.
- [135] H. Jung, B. Friedman, W. Hwang, A. Copping, R. Branch, Z.D. Deng, Self-powered arctic satellite communication system by harvesting wave energy using a triboelectric nanogenerator, *Nano Energy* 114 (2023) 108633, <https://doi.org/10.1016/j.nanoen.2023.108633>.
- [136] X. Chen, L. Gao, J. Chen, S. Lu, H. Zhou, T. Wang, A. Wang, Z. Zhang, S. Guo, X. Mu, Z.L. Wang, Y. Yang, A chaotic pendulum triboelectric-electromagnetic hybridized nanogenerator for wave energy scavenging and self-powered wireless sensing system, *Nano Energy* 69 (2020) 104440, <https://doi.org/10.1016/j.nanoen.2019.104440>.
- [137] J. Sun, L. Zhang, S. Gong, J. Chen, H. Guo, Device physics and application prospect of the emerging high-voltage supply technology arising from triboelectric nanogenerator, *Nano Energy* 119 (2024) 109010, <https://doi.org/10.1016/j.nanoen.2023.109010>.
- [138] S.A. Graham, S.C. Chandrarathna, P. Manchi, M.V. Paranjape, J.K. Lee, J. Lee, J. S. Yu, Triboelectric charge modulation to understand the electrification process in nanogenerators combined with an efficient power management system for IoT applications, *Nano Energy* 111 (2023) 108413, <https://doi.org/10.1016/j.nanoen.2023.108413>.
- [139] Y. Zhou, P. Zhang, J. Li, X. Mao, Recent progress of triboelectric nanogenerator-based power management and information processing circuit, *Mater. Today Sustain.* 23 (2023) 100426, <https://doi.org/10.1016/j.mtsust.2023.100426>.
- [140] C. Song, X. Zhu, M. Wang, P. Yang, L. Chen, L. Hong, W. Cui, Recent advances in ocean energy harvesting based on triboelectric nanogenerators, *Sustain. Energy Technol. Assess.* 53 (2022) 102767, <https://doi.org/10.1016/j.seta.2022.102767>.
- [141] Y. Mi, Y. Lu, X. Wang, Z. Zhao, X. Cao, N. Wang, From Triboelectric Nanogenerator to Uninterrupted Power Supply System. The Key Role of Electrochemical Batteries and Supercapacitors, 2022.
- [142] C. Fang, T. Tong, T. Bu, Y. Cao, S. Xu, Y. Qi, C. Zhang, Overview of power management for triboelectric nanogenerators, *Adv. Intell. Syst.* 2 (2020) 2070020, <https://doi.org/10.1002/aisy.202070020>.
- [143] H. Qin, G. Cheng, Y. Zi, G. Gu, B. Zhang, W. Shang, F. Yang, J. Yang, Z. Du, Z. L. Wang, High energy storage efficiency triboelectric nanogenerators with unidirectional switches and passive power management circuits, *Adv. Funct. Mater.* 28 (2018) 1805216, <https://doi.org/10.1002/adfm.201805216>.
- [144] J. Gravesen, M. Willatzen, J. Shao, Z.L. Wang, Modeling and optimization of a rotational symmetric spherical triboelectric generator, *Nano Energy* 100 (2022) 107491, <https://doi.org/10.1016/j.nanoen.2022.107491>.
- [145] J. Gravesen, M. Willatzen, J. Shao, Z.L. Wang, Modeling and optimization of a spherical triboelectric generator, *Nano Res.* 16 (2023) 11925-11931, <https://doi.org/10.1007/s12274-023-5745-4>.
- [146] J. Gravesen, M. Willatzen, J. Shao, Z.L. Wang, Energy optimization of a mirror-symmetric spherical triboelectric nanogenerator, *Adv. Funct. Mater.* 32 (2022) 2110516, <https://doi.org/10.1002/adfm.202110516>.
- [147] J. Gravesen, M. Willatzen, J. Shao, Z.L. Wang, Quantitative Calculation of Output Power and Spherical Triboelectric Nanogenerators, in: Z.L. Wang, Y. Yang,

J. Zhai, J. Wang (Eds.), *Handbook of Triboelectric Nanogenerators*, Springer International Publishing, Cham, 2023, pp. 1-39.

- [148] M.M.M. Kuypers, H.K. Marchant, B. Kartal, The microbial nitrogen-cycling network, *Nat. Rev. Microbiol.* 16 (2018) 263-276, <https://doi.org/10.1038/nrmicro.2018.9>.

- [149] X. Liang, S. Liu, H. Yang, T. Jiang, Triboelectric nanogenerators for ocean wave energy harvesting: unit integration and network, *Construction* (2023).



Junjie Cui received his Ph. D. degree from School of Materials Science and Engineering in 2020, from Inner Mongolia University of Technology, China. Currently, he is a lecturer at the Inner Mongolia University of Science and Technology. He joined Inner Mongolia University of Science and Technology from September 2009 as a faculty member. His research interests include high-entropy ocean wave energy and breeze energy harvesting using triboelectric nanogenerators and self-powered sensing system.



Hao Li is currently a doctoral student at the University of Chinese Academy of Sciences. His research focuses on friction nanogenerators for energy harvesting and self-powered sensing system.



Dr. Baodong Chen is a professor in Beijing Institute of Nanoenergy and Nanosystems, Chinese Academy of Sciences. He received his PHD degree from School of Materials Science and Engineering in 2015, from Inner Mongolia University of Technology, China. Prior to joining the faculty at BINN (CAS) in 2018, he was a postdoctoral fellow at National Center for Nanoscience and Technology. His research interests include triboelectric nanogenerators, self-powered systems, and 2D and 3D printed flexible electronics.



Zhong Lin Wang is the Hightower Chair in Materials Science and Engineering and Regents' Professor at Georgia Tech, and the chief scientist and director of the Beijing Institute of Nanoenergy and Nanosystems, Chinese Academy of Sciences. His discovery and breakthroughs in developing nanogenerators and self-powered systems establish the principle and technological road map for harvesting mechanical energy from environmental and biological systems for powering personal electronics and future sensor networks. He coined and pioneered the field of piezotronics and piezophotonics.